



Metformin and Trehalose-Modulated Autophagy Exerts a Neurotherapeutic Effect on Parkinson's Disease

Yareth Gopar-Cuevas¹ · Odila Saucedo-Cardenas¹ · Maria J. Loera-Arias¹ · Roberto Montes-de-Oca-Luna¹ · Humberto Rodriguez-Rocha¹ · Aracely Garcia-Garcia¹

Received: 1 May 2023 / Accepted: 20 July 2023 / Published online: 5 August 2023
© The Author(s), under exclusive licence to Springer Science+Business Media, LLC, part of Springer Nature 2023

Abstract

Since the number of aged people will increase in the next years, neurodegenerative diseases, including Parkinson's Disease (PD), will also rise. Recently, we demonstrated that autophagy stimulation with rapamycin decreases dopaminergic neuronal death mediated by oxidative stress in the paraquat (PQ)-induced PD model. Assessing the neurotherapeutic efficacy of autophagy-inducing molecules is critical for preventing or delaying neurodegeneration. Therefore, we evaluated the autophagy inducers metformin and trehalose effect in a PD model. Autophagy induced by both molecules was confirmed in the SH-SY5Y dopaminergic cells by detecting increased LC3-II marker and autophagosome number compared to the control by western blot and transmission electron microscopy. Both autophagy inducers showed an antioxidant effect, improved mitochondrial activity, and decreased dopaminergic cell death induced by PQ. Next, we evaluated the effect of both inducers in vivo. C57BL6 mice were pretreated with metformin or trehalose before PQ administration. Cognitive and motor deteriorated functions in the PD model were evaluated through the nest building and the gait tests and were prevented by metformin and trehalose. Both autophagy inducers significantly reduced the dopaminergic neuronal loss, astrocytosis, and microgliosis induced by PQ. Also, cell death mediated by PQ was prevented by metformin and trehalose, assessed by TUNEL assay. Metformin and trehalose induced autophagy through AMPK phosphorylation and decreased α -synuclein accumulation. Therefore, metformin and trehalose are promising neurotherapeutic autophagy inducers with great potential for treating neurodegenerative diseases such as PD.

Keywords Metformin · Trehalose · Autophagy · Parkinson's disease · Dopaminergic neurons · Paraquat

Highlights

Autophagy inducers metformin and trehalose in a Parkinson's disease model induced with paraquat prevented:

- Oxidative stress and mitochondrial dysfunction
- PQ-induced autophagy deterioration
- Cognitive and motor dysfunction
- Loss of dopaminergic neurons and oligodendrocytes
- Astrocytosis and microgliosis
- α -synuclein accumulation

✉ Humberto Rodriguez-Rocha
humberto.rodriguezrc@uanl.edu.mx

✉ Aracely Garcia-Garcia
aracely.garciagr@uanl.edu.mx

¹ Departamento de Histología, Facultad de Medicina, Universidad Autónoma de Nuevo León, Francisco I. Madero S/N, 64460 Monterrey, Nuevo León, Mexico

Introduction

The current life expectancy worldwide is 73 years [1], and the number of aged people will increase significantly in the following years [2], which is associated with a more significant increase in the presence of neurodegenerative diseases, such as Parkinson's disease (PD). PD is a neurological and motor disorder characterized by bradykinesia, rigidity, postural instability, and tremor, symptoms caused by dopaminergic neuronal death in the substantia nigra pars compacta, resulting in dopaminergic denervation of the striatum [3, 4]. Epidemiological studies have demonstrated that environmental exposure to paraquat (PQ), which is widely used as an herbicide, increases the risk of developing PD [5]. PQ toxicity is due to its ability to enter a redox cycle that leads to NADPH consumption and PQ reduction, forming the free radical PQ, which in turn can spontaneously react with oxygen, leading to the formation of superoxide anion,

peroxynitrite, hydrogen peroxide, and hydroxyl radical, thus producing mitochondrial and cytoplasmic oxidative stress followed by cell death [6, 7]. Previously, we reported that autophagy is impaired by PQ exposure [8], which is consistent with autophagic vesicle accumulation in PD patients' postmortem brains [9, 10].

Autophagy consists of cellular components degradation through lysosomal hydrolases for subsequent molecule recycling [11]. Autophagy plays an essential role in the proper functioning of the central nervous system (CNS) since its deficiency leads to neurodegeneration [12–14]. Recent evidence has highlighted the role played by autophagy in mitochondrial quality control and its relationship with neurodegenerative diseases like PD [15]. Given the importance of this process, we consider that the stimulation of autophagy may prevent PD development. Indeed, we previously demonstrated that autophagy induction with rapamycin decreases dopaminergic neuronal death mediated by oxidative stress in the paraquat (PQ)-induced PD model [16]. Rapamycin is the best-characterized autophagy inducer and has been the most widely used [17, 18], showing positive effects in experimental neurodegenerative diseases [19]. However, it was recently found that rapamycin administration was associated with affected microglial activity and increased β -amyloid plaques in an Alzheimer's disease model [20]. Therefore, assessing the neurotherapeutic efficacy of other autophagy-inducing molecules, such as metformin and trehalose, is critical for preventing or delaying neurodegeneration.

Metformin is a hypoglycemic agent widely used to treat type 2 diabetes mellitus [21]. In addition, metformin induces autophagy through an AMPK-dependent mechanism causing a starvation state by inhibiting complex 1 of the respiratory chain and mitochondrial glycerophosphate dehydrogenase (mGPDH) [22]. Complex 1 inhibition decreases NADH oxidation, proton pumping across the inner mitochondrial membrane, and the oxygen consumption rate, resulting in a lower proton gradient and reduced ATP synthesis. Furthermore, metformin suppresses gluconeogenesis by inhibiting mGPDH [23, 24].

On the other hand, trehalose is a disaccharide formed from two glucose molecules, where the α -type glycosidic linkage involves the hydroxyl groups of the two anomeric carbons [25]. Trehalose induces autophagy through mTOR-dependent and independent pathways. Trehalose inhibits glucose transporters (GLUT), generating a state similar to starvation, which activates autophagy through AMPK and ULK1 [26]. In addition, trehalose can induce autophagy, causing rapid and transient lysosomal enlargement and membrane permeabilization with subsequent TFEB nuclear translocation, stimulating lysosome biogenesis [27].

To date, no notable side effects of metformin and trehalose that affect patients' quality of life have been reported. In addition, more and more health benefits are attributed to

them [22, 28–30], which is why we consider that they have promising potential as therapeutic alternatives for treating patients with PD.

Materials and Methods

Cell Culture

Human dopaminergic neuroblastoma cell line SH-SH5Y was obtained from the American Type Culture Collection (CRL-2266, ATCC, Manassas, VA). Cells were cultured in DMEM/F12 medium (10–092-CMR, Corning Inc., Corning, NY) containing 10% heat-inactivated fetal bovine serum (35–010-cv, Thermo Fisher Scientific, Waltham, MA), 100 units/mL penicillin–streptomycin (30–004-Cl, Corning Inc.) in a humidified 37° C incubator with 5% CO₂. Cells were treated with PQ (1,1'-dimethyl-4,4'-bipyridinium dichloride) at 0.5 mM (36,541, Merck Millipore, Burlington, MA) for 24 h (oxidative stress assays and MTT assay) or 48 h (cell death assays). Metformin 1 mM and 2.5 mM (D150959, Merck Millipore), Trehalose 100 mM (182,551,000, Thermo Fisher Scientific), and Rapamycin 10 μ M (R-5000, LC Laboratories, Woburn, MA) were used to stimulate autophagy, 1 h before PQ treatment. For autophagy flux experiments, 40 μ M chloroquine (CQ) was added 4 h before harvesting cells.

Transmission Electron Microscopy (TEM)

Cells were fixed with 2.5% glutaraldehyde in 0.1 M sodium cacodylate (pH 7.4) for 2 h at room temperature. Fixed cells were collected and post-fixed with 1% osmium tetroxide (OsO₄) in sodium cacodylate and counterstained in 1% uranyl nitrate. The pellets were dehydrated through a graduated acetone series and embedded in Epon 812 resin (14,120, Electron Microscopy Sciences, Hatfield, PA) for sectioning. The resin blocks were cut with a diamond blade to obtain thin sections with a thickness between 60 and 80 nm, which were placed on a copper grid. The ultrastructure of cells was observed from thin sections under a transmission electron microscope (EM 109, Carl Zeiss, Oberkochen, Germany), and images were collected with a Dage-MTI CCD-72 Camera and VLC media player software. Autophagosome presence was evaluated by morphometric analysis in fifty cells per treatment.

Western Immunoblotting (WB)

Cells were lysed in radioimmunoprecipitation assay (RIPA) buffer (20 mM Tris–HCl, 150 mM NaCl, 1 mM Na₂EDTA, 1 mM ethylene glycol tetraacetic acid (EGTA), 1% Triton X-100) containing Halt Protease Inhibitor Cocktail (78,430,

Thermo Fisher Scientific). Samples were sonicated and centrifuged, and pellets were discarded. Thirty-five to 50 μg of protein per sample were loaded and separated by SDS–polyacrylamide gel electrophoresis and transferred to PVDF membranes. Blots were incubated at 4 °C overnight with the appropriate primary antibody (1:1000): rabbit anti-LC3 (L7543, Merck Millipore) or rabbit anti- β -actin (sc-2357, Santa Cruz Biotechnology, Dallas, TX) to verify equal protein loading. Peroxidase-conjugated secondary anti-rabbit at 1:2000 dilution (sc-2004, Santa Cruz Biotechnology) was used, and bands were detected using SuperSignal West Pico Plus Chemiluminescent Substrate (34,580, Thermo Fisher Scientific). Densitometry analysis of immunoblots was performed using ImageJ (NIH) v3.91 software (<http://rsb.info.nih.gov/ij>) and normalized to β -actin. Western blots were representative of 3 independent experiments.

Cytoplasmic Oxidative Stress

Cells were incubated with dihydroethidium fluorescent dye (DHE, D11347, Thermo Fisher Scientific) at 10 μM for 15 min (ex. 490 nm, em. 570 nm), harvested with trypsin and resuspended in PBS 1X. Finally, cells were evaluated by flow cytometry (Muse Cell Analyzer, Merck Millipore).

Mitochondrial Oxidative Stress

Cells were incubated with MitoTracker Red CM-H₂XROS fluorescent dye (M7513, Thermo Fisher Scientific) at 500 nM for 30 min. (ex. 580 nm, em. 600 nm), nuclei were stained with VECTASHIELD Antifade Mounting Medium with DAPI (H1200, Thermo Fisher Scientific). The mitochondrial oxidative stress was analyzed by fluorescence microscopy. Images were collected on a Nikon Eclipse 50i fluorescence microscope (Nikon, Melville, NY) and analyzed using ImageJ software.

Immunofluorescence

Cells SH-SY5Y were fixed with methanol and blocked with 10% normal horse serum (16,050–122, Thermo Fisher Scientific), then were incubated with rabbit anti-PrxSO₃ antibody (ab16830, Abcam, Cambridge, MA) overnight at 4 °C. After rinsing, sections were incubated with secondary Alexa 488 anti-rabbit (ab150080, Abcam) for 1 h at RT.

At the end of the experimental animal model (described below), mice were anesthetized with an intraperitoneal injection of 10 mg/kg xylazine (Q7833099, PiSA Labs, General Escobedo, Mexico) and 100 mg/kg ketamine (Q7833028, PiSA Labs). Afterward, mice were perfused intracardially with 4% paraformaldehyde (PFA). Brains were removed and post-fixed for 24 h in 4% PFA. Midbrains were cut into 5 μm coronal sections using a sliding microtome. Sections

were blocked with 10% normal horse serum (16,050–122, Thermo Fisher Scientific) and incubated with primary antibody (1:1000): mouse anti-TH antibody (sc-25269, Santa Cruz Biotechnology), rabbit anti-CNPase (PA5-27,972, Thermo Fisher Scientific), rabbit anti-GFAP (ab7260, Abcam), rabbit anti-Iba-1 (178,847, Abcam), rabbit anti-AMPK alpha 1 (phospho T183) + AMPK alpha 2 (phospho T172) (ab23875, Abcam), rabbit anti-LC3 (L7543, Merck Millipore) or mouse anti- α -synuclein (sc-12767, Santa Cruz Biotechnology) overnight at 4 °C. After rinsing, sections were incubated with secondary antibody (1:1000): Alexa 488 anti-mouse (A-11001, Thermo Fisher Scientific), Alexa 488 anti-rabbit (A-11008, Thermo Fisher Scientific) or Alexa 568 anti-rabbit (A-11011, Thermo Fisher Scientific) for 1 h at RT.

Sections were mounted with VECTASHIELD Antifade Mounting Medium with DAPI (H1200, Thermo Fisher Scientific). Images were obtained on a Nikon Eclipse 50i fluorescence microscope (Nikon, Melville, NY) and analyzed using ImageJ software. The acquisition parameters were kept the same for each marker, including the exposure time, laser intensity, gain adjustment, and image magnification. We evaluated three random fields per section from three subjects per group. MitoTracker Red CM-H₂XROS and PrxSO₃ were analyzed with the corrected total cell fluorescence (CTCF) obtained with the following formula: $\text{CTCF} = \text{Integrated Density} - (\text{Area of selected cell} \times \text{Mean fluorescence of background readings})$. Dopaminergic neurons', astrocytes, and α -synuclein were evaluated by counting the number of positive cells per field. For the microglia and pAMPK detection, the total fluorescence intensity of the field was measured.

MTT Assay

Mitochondrial activity dysfunction was assessed as a marker of cytotoxicity by measuring the conversion of the tetrazolium salt MTT (3-[4,5-dimethylthiazol-2-yl]-2,5-diphenyltetrazolium bromide) (M2128, Merck Millipore) to formazan. A solution of MTT at the final concentration of 5 mg/mL was added at the end of treatment and incubated for 2 h at 37 °C. Then, lysis buffer (4 mM HCl, 0.1% Nonidet P-40) was added to solubilize MTT tetrazolium crystal. Finally, the optical density was determined at 590 nm using iMark microplate reader (Bio-Rad, Hercules, CA).

Trypan Blue Exclusion Assay

Representative microphotographs of treated cells (48 h) were acquired using an inverted microscope. Afterward, adherent cells were detached by trypsinization and washed with PBS. Cells were stained with trypan blue (15,250–061, Thermo Fisher Scientific) at a final concentration of 0.2% for 5 min

and counted using an automated cell counter (TC20, Bio-Rad, Hercules, CA). The viable cells (non-stained) with the intact membrane exclude the dye, while dead cells take up the coloring blue reagent.

Apoptosis Assay

Apoptosis was determined by using the Muse Annexin V & Dead Cell Kit (MCH100105, Merck Millipore). This assay is based on the ability of Annexin V to bind to phosphatidylserine, a marker of apoptosis, and the uptake of 7-amino actinomycin D (7-AAD) as a marker for loss of plasma membrane integrity. Data are represented as a percentage of early apoptosis and late apoptosis/dead. Early apoptotic cells have Annexin V-positive and 7-AAD-negative staining, while late-apoptotic/dead cells are both Annexin V and 7-AAD-positive.

Parkinson's Disease Animal Model

C57BL/6 J male mice (8–10 weeks old) (Circulo ADN, Mexico City) were divided into 8 groups formed by 3 subjects each: 1) Control, injected with PBS; 2) Rapamycin; 3) Trehalose; 4) Metformin; 5) PQ; 6) Rapamycin + PQ; 7) Trehalose + PQ, and 8) Metformin + PQ. Rapamycin (1 mg/Kg) and PQ (10 mg/Kg) were prepared in PBS and administered intraperitoneally. Metformin (500 mg/Kg) and trehalose (3.2 g/Kg) were prepared daily and administered orally in the drinking water ad libitum. The autophagy inducers' doses were calculated considering the mice's average daily water consumption (4 mL). Rapamycin was administered every other day. PQ (AC227320010, Thermo Fisher Scientific) was used to induce the experimental PD model and was applied twice a week for 7 consecutive weeks. Autophagy inducers were administered one week before PQ treatment and for 7 consecutive weeks. Mice were maintained on a 12-h light–dark cycle, with free access to Prolab RMH 2500 pellets (5P14, LabDiet, St. Louis, MO) and water. The body weight of all mice was recorded weekly. All experiments were conducted under the Mexican Official Norm “NOM-062-ZOO-1999” (De Aluja, 2002) and the Institutional Committee for the Care and Use of Laboratory Animals (Comite Institucional para el Cuidado y Uso de los Animales de Laboratorio, CICUAL), and approved by the Ethical Committee of Facultad de Medicina of Universidad Autonoma de Nuevo Leon (registration number HT19-00002).

Nest-Building Test

Cognitive function can be measured through social behaviors directly linked to reproductive function and parenting. Nests are essential in conserving heat, reproduction, and shelter for small rodents. To perform the nest-building test,

the mice received 5 g of compressed cotton, and the evaluation was made based on a previously reported nest-scoring system [31]. Briefly, the nests were evaluated considering the height and closure of the walls surrounding the nest cavity. Higher scores indicated higher quality nests, equivalent to typical behavior (score of 5 = full dome-shaped nest), while those with lower scores corresponded to poor quality nests and indicated abnormal behavior (score of 4 = incomplete dome-shaped nest; a score of 3 = cup-shaped nest; a score of 2 = flat nest; and scores of 1 and 0 were referred to disturbed and undisturbed nesting material, respectively).

Gait Test

Mice's motor function was assessed through the gait test [32] by painting their front and rear paws with red and blue non-toxic washable paint, respectively. This test takes advantage of the natural behavior of the mouse and its affinity for small dark places, is sensitive enough to detect early changes in gait, and due to its non-invasive approach, allows evaluation of groups throughout the life or evolution of the disease. Before starting the test, the mice were acclimatized for thirty minutes. Afterward, mice were allowed to walk through a tunnel on a sheet of paper. The tunnel had the necessary dimensions that allowed the mice to walk comfortably and take enough steps (>4) to measure the gait. The parameters that were measured in the paws printed patterns were each mouse's hindlimbs and forelimbs stride length and stride width.

TUNEL Assay

Terminal deoxynucleotidyl transferase dUTP nick end labeling (TUNEL) assay was performed using In Situ BrdU-Red DNA Fragmentation (TUNEL) Assay Kit (ab66110, Abcam), according to the manufacturer's instructions. Briefly, tissue sections were incubated with proteinase K 20 µg/mL for 5 min at RT, followed by DNA Labeling Solution for 1 h at 37 °C, and finally, Anti-BrdU-Red antibody for 30 min at room temperature. Sections were mounted with VECTASHIELD Antifade Mounting Medium with DAPI (H1200, Thermo Fisher Scientific). Images were obtained on a Nikon Eclipse 50i fluorescence microscope (Nikon, Melville, NY) and analyzed using ImageJ software.

Statistical Analysis

All replicates of the experiment were independent and performed on separate days. Two-way ANOVA was used to determine statistical significance, followed by Student's t-test when statistical significance was found between groups and analyzed using the statistical software Prism 6 (GraphPad Software, San Diego, CA). A probability value of $p < 0.05$

was considered statistically significant. Data were plotted as mean values of at least 3 independent experiments (for the cellular model) or 3 subjects (for the animal model) \pm SD using the same statistical package for data analysis. The plots and WB presented are representatives of at least 3 independent experiments.

Results

Autophagy Inducers Metformin and Trehalose are Harmless to Dopaminergic Cells

First, the effect of autophagy inducers on SH-SY5Y dopaminergic cells was evaluated to ensure that the molecules used were not toxic. The cells were treated with metformin (1, 2.5, 5, and 10 mM), trehalose (50, 100, and 150 mM), or rapamycin (10 μ M) as a positive control to induce autophagy. Cell morphology was evaluated by direct observation of cell cultures through an inverted microscope; cell morphology remained unchanged in response to the different concentrations of metformin (Supplementary Fig. 1A) and trehalose (Supplementary Fig. 1D) compared to the control that received no treatment and to rapamycin (positive control). Most cells were attached to the culture dish and showed spindle-shaped with cytoplasmic ramifications, and in a smaller proportion, rounded floating cells were observed, representing the basal cell death levels. Subsequently, trypan blue exclusion assessed viability, which was not significantly affected in response to metformin (Supplementary Fig. 1B) or trehalose (Supplementary Fig. 1E) after 48 h of treatment. These results indicate that none of the evaluated concentrations of metformin and trehalose are toxic to cells.

Next, to establish the metformin and trehalose optimal dose for autophagy induction, the LC3-II autophagy marker was evaluated through western blot. LC3-II increased with as low as 1 mM metformin at 24 h of treatment compared to rapamycin, and no significant increase was observed at higher concentrations (2.5, 5 y 10 mM) (Supplementary Fig. 1C). Trehalose increased LC3-I to LC3-II conversion, with the highest effect at 100 mM at 24 h (Supplementary Fig. 1F). Metformin at 1 mM and trehalose at 100 mM were used in the following experiments unless stated, as cell morphology and viability were not affected, and autophagy was effectively induced.

Metformin and Trehalose Prevent Autophagy Disruption Mediated by PQ

Alterations in the autophagy process have been reported in PD patients' brains [10], and PQ has an inhibitory effect on the autophagy mechanism, which is prevented by rapamycin [8]. Therefore, we evaluated whether metformin and

trehalose may also prevent PQ-mediated autophagy disruption. The presence of autophagic vesicles in different maturation degrees was evaluated through transmission electron microscopy (TEM) after pre-treatment with autophagy inducers, followed by PQ for 24 h. Double membrane structures with heterogeneous content (autophagosomes) and single membrane content (autolysosomes) were identified (Fig. 1A). Basal autophagy levels are shown in control cells (untreated cells). An increase in the number of autophagic vesicles was observed in response to all autophagy inducers. PQ-treated cells had large autophagosomes with cytoplasmic content, consistent with autophagy flux blockage and the subsequent autophagosome accumulation. Autophagy stimulation before exposure to PQ decreased the size of autophagosomes, which were in different degrees of maturation compared to cells treated only with PQ. Also, 50 cells per treatment were evaluated for the presence of autophagosomes and normalized to the control (Fig. 1B). Thus, the autophagy stimulation was confirmed in response to rapamycin, metformin, or trehalose compared to the control.

Next, autophagy flux was evaluated using chloroquine (CQ), followed by LC3-II detection by western blot (Fig. 1C and 1D). In neutral pH, CQ diffuses freely through cell membranes, while in an acid medium, it is protonated and remains trapped in lysosomes, leading to increased lysosomal pH, impaired lysosomal digestion, and autophagosome accumulation, blocking autophagy flux. Compared to the control, an increase in LC3-II was detected in the cells treated with metformin (Fig. 1C) or trehalose (Fig. 1D). PQ-treated cells showed a decrease in LC3-II, consistent with autophagy flux disruption. Autophagy induction before PQ treatment prevented impairment of autophagy flux, showing higher levels of LC3-II than cells that received only PQ. In the presence of CQ, both autophagy inducers increased LC3-II compared to CQ alone. PQ inhibitory effects on autophagy were confirmed in the presence of CQ by showing lower LC3-II levels than CQ. Therefore, metformin and trehalose are effective autophagy inducers and prevent PQ-mediated autophagy blockage.

Metformin and Trehalose Exert an Antioxidant Effect on Mitochondrial Oxidative Stress

Studies in brains obtained from autopsies of PD patients demonstrated oxidative damage in lipids, proteins, and DNA [33–35]. Furthermore, oxidative stress has been related to mitochondrial dysfunction because of the decreased electron transport chain activity observed in the neurons of the substantia nigra pars compacta of PD patients [36, 37]. Thus, we evaluated the reactive oxygen species (ROS) levels in the cytoplasmic and mitochondrial compartments. Metformin and trehalose effect on PQ-induced cytoplasmic oxidative stress was evaluated by flow cytometry using

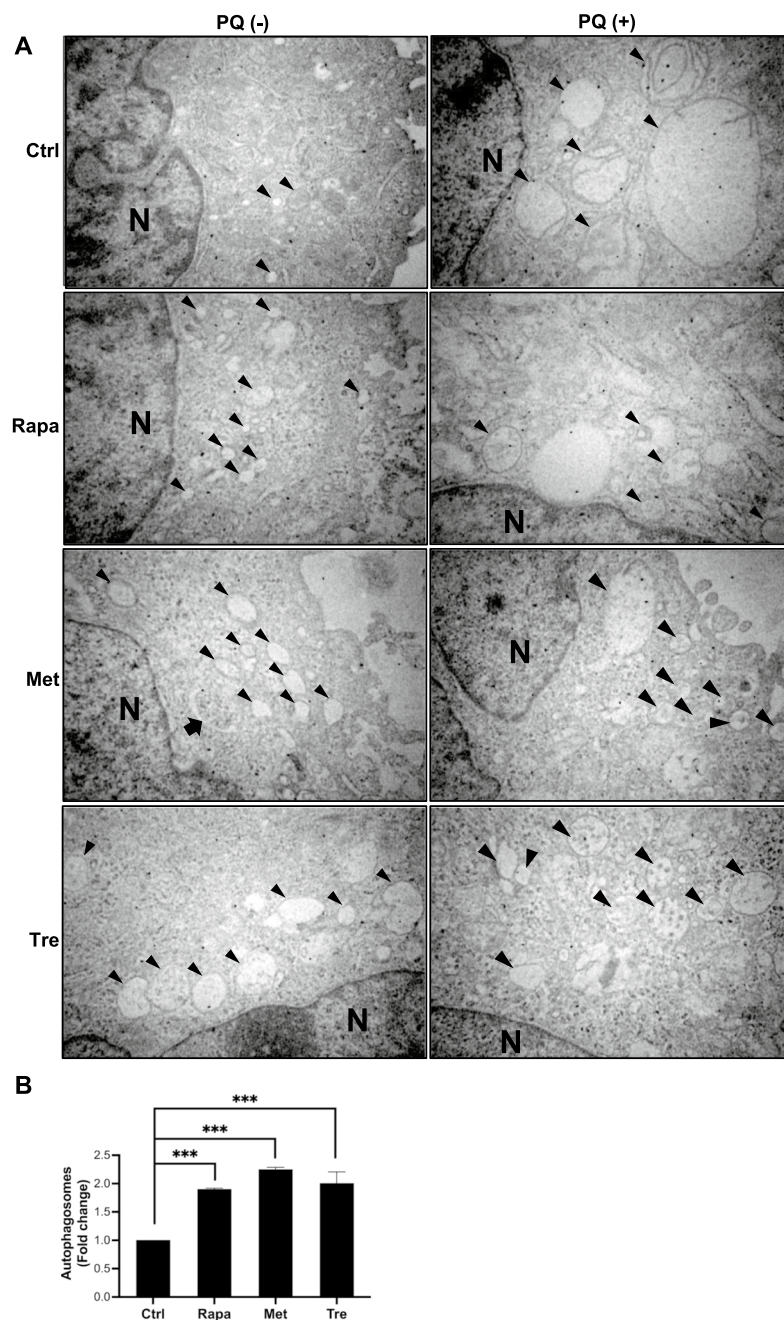


Fig. 1 Autophagy induced by metformin and trehalose prevents autophagosome alterations induced by PQ. SH-SY5Y cells were pre-treated with rapamycin (10 μ M), metformin (1 mM), or trehalose (100 mM) 1 h before PQ (0.5 mM) treatment, and cells were analyzed after 24 h. **A** Electron microphotographs (12,000 \times). Untreated cells show basal levels of autophagy. PQ-treated cells had large autophagosomes (double-membrane vesicles) with cytoplasmic content, consistent with autophagy flux impairment. Cells pre-treated with the autophagy inducers showed an increased number of autophagosomes. Autophagy stimulation before PQ exposure decreased the alterations produced by PQ. **B** Autophagosomes were evaluated by morphometric analysis using TEM, where 50 cells per treatment were analyzed. Results are expressed as fold change and were normalized to the control. An increased number of autophagic vesicles was

observed in response to all autophagy inducers compared to the control. **C** and **D** Western blot of autophagy marker LC3-II. We evaluated the autophagy flux using chloroquine (CQ). Metformin (**C**) and trehalose (**D**) with CQ increased LC3-II. PQ-treated cells showed a decrease in the LC3-II protein compared to the CQ, which is consistent with the autophagy flux blockage and the autophagosome accumulation in the cytoplasm. Autophagy stimulation before PQ treatment induced higher LC3-II levels than cells treated with CQ. β -actin was used as a loading control. Densitometry values are shown below each line. Ctrl, control; Rapa, rapamycin; Met, metformin; Tre, trehalose; PQ, paraquat. The (*) indicates autophagic vesicles, (N) nucleus, and (m) mitochondria. A probability value of $p < 0.05$ was considered statistically significant; *** $p < 0.001$

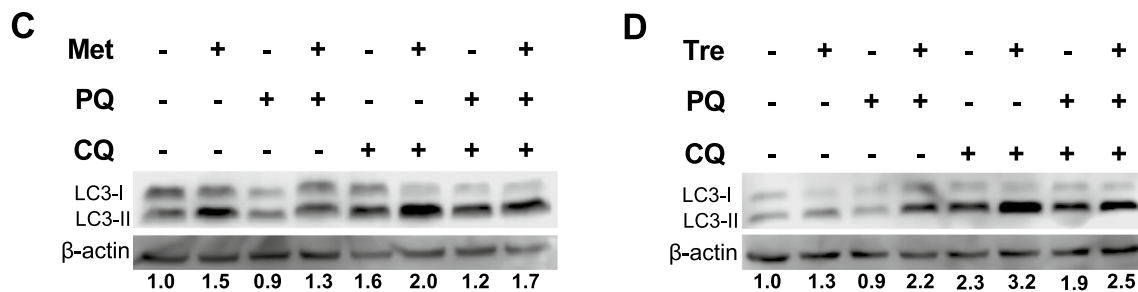


Fig. 1 (continued)

dihydroethidium (DHE), which, once oxidized to ethidium, intercalates in DNA and exhibits a bright red fluorescence. Rapamycin was used as a positive control of autophagy induction, which had an antioxidant effect on PQ-induced oxidative stress (Fig. 2A, representative histograms), as previously reported [38]. Metformin at the concentration of 1 mM did not significantly affect PQ-induced oxidative stress, so we increased the concentration to 2.5 mM expecting an antioxidant effect. However, this metformin concentration notably increased basal and PQ-induced oxidative stress (Fig. 2B). Furthermore, trehalose did not affect oxidative stress produced by PQ (Fig. 2B).

Next, mitochondrial ROS generation was analyzed by fluorescence microscopy using Mitotracker™ Red CM-H₂XRos dye, which, once oxidized, exhibits a bright red fluorescence (Fig. 2C). DAPI was used to label the nuclei in blue. The fluorescence intensity of Mitotracker™ Red CM-H₂XRos was quantified (Fig. 2D). Autophagy inducers did not affect basal levels of mitochondrial oxidative stress. PQ treatment increased mitochondrial oxidative stress, which was decreased by pre-treatment with autophagy inducers. These results indicate that metformin and trehalose exert an antioxidant effect on mitochondrial oxidative stress.

High ROS levels and reduced antioxidant enzyme activity in PD patients' dopaminergic neurons lead to oxidative stress and, ultimately, neuroinflammation [39]. Then, we evaluated the effect of autophagy inducers on PQ-induced alterations in the redox state of peroxiredoxins (Prxs), a group of antioxidant enzymes capable of reducing hydrogen peroxide, peroxynitrite, and other organic peroxides that cause cellular damage [40], and which hyperoxidation reflects a highly oxidizing environment [41]. Previously, we reported Prxs hyperoxidation (PrxSO₃) in response to PQ and its prevention through autophagy prestimulation with rapamycin [16, 38]. Immunofluorescence was performed with a specific antibody for the detection of PrxSO₃ (green signal), and DAPI was used to label the nuclei (Fig. 2E). The fluorescence intensity of PrxSO₃ immunodetection was quantified (Fig. 2F). Rapamycin, metformin, or trehalose treatment did not affect basal oxidative stress levels. In contrast, PQ caused a significant increase in the positive signal

for PrxSO₃ compared to the control. Metformin treatment had no effect on PQ-induced PrxSO₃. However, trehalose significantly decreased PQ-mediated Prxs hyperoxidation. Therefore, metformin and trehalose decreased mitochondrial oxidative stress, and only trehalose reduced PrxSO₃ induced by PQ.

Autophagy Stimulated by Metformin and Trehalose has a Protective Effect on PQ-Mediated Toxicity

Because the main pathophysiological feature of PD is the selective death of dopaminergic neurons [42], we evaluated dopaminergic cell viability by trypan blue exclusion. After 48 h of treatment, the cell morphology was evaluated directly from the culture plate through an inverted microscope. The cells without treatment (control) were mainly adherent with spindle-shaped and cytoplasmic ramifications (Fig. 3A). A small proportion of rounded shape cells were floating in the culture medium, corresponding to basal death. In response to PQ, cells were primarily rounded and floating in the medium. When cells received an autophagy inducer followed by PQ treatment, floating cells decreased, and the cell morphology was preserved as in the control cells.

The main target of PQ within the cell is the mitochondria [43], as PQ enters a vicious Redox cycle interfering with the electron transport chain by inhibiting NADP reduction to NADPH [5, 44]. Then, we assessed the effect of metformin and trehalose-induced autophagy on mitochondrial activity by MTT assay. Autophagy inducers did not alter mitochondrial activity (Fig. 3B). PQ-treated cells had significantly less mitochondrial activity than the control, whereas when autophagy was stimulated with rapamycin, metformin, or trehalose prior to PQ treatment, mitochondrial activity was significantly increased.

Trypan blue exclusion confirmed the previous results (Fig. 3C). PQ decreased cell viability compared to the control and significantly increased when autophagy was prestimulated, indicating a protective effect.

PQ induces caspase-dependent apoptosis [8, 45], and we previously demonstrated that rapamycin protects dopaminergic cells from PQ-induced apoptosis [16]. We assessed

Fig. 2 Induction of autophagy decreases mitochondrial oxidative stress and peroxiredoxins hyperoxidation mediated by PQ. Cells were pre-treated with rapamycin (10 μ M), metformin (1 and 2.5 mM), or trehalose (100 mM), 1 h before PQ (0.5 mM) treatment and analyzed at 24 h. **A** Harvested cells were incubated with DHE dye (1 μ L / mL) for 15 min and analyzed by flow cytometry. Rapamycin showed an antioxidant effect on oxidative stress induced by PQ. Metformin increased, and trehalose did not affect oxidative stress induced by PQ. **B** Statistical analysis of flow cytometry. **C** Cells were incubated with Mitotracker Red CM-H₂XRos dye (500 nM) for 30 min and analyzed by fluorescence microscopy. PQ increased mitochondrial oxidative stress, which was decreased by pre-treatment with rapamycin, metformin, or trehalose. **D** Fluorescence intensity quantification of Mitotracker Red CM-H₂XRos. **E** Peroxiredoxin hyperoxidation was detected with an anti-PrxSO₃ antibody. PQ induced peroxiredoxins hyperoxidation, which was decreased by pre-treatment with rapamycin and trehalose, but not metformin. **F** Fluorescence intensity quantification of peroxiredoxin hyperoxidation. DAPI was used as a nuclear marker. The values were normalized to the control. Ctrl, control; Rapa, rapamycin; Met, metformin; Tre, trehalose; PQ, paraquat. A probability value of $p < 0.05$ was considered statistically significant; * $p < 0.05$; ** $p < 0.01$; *** $p < 0.001$; **** $p < 0.0001$; ns, not significant

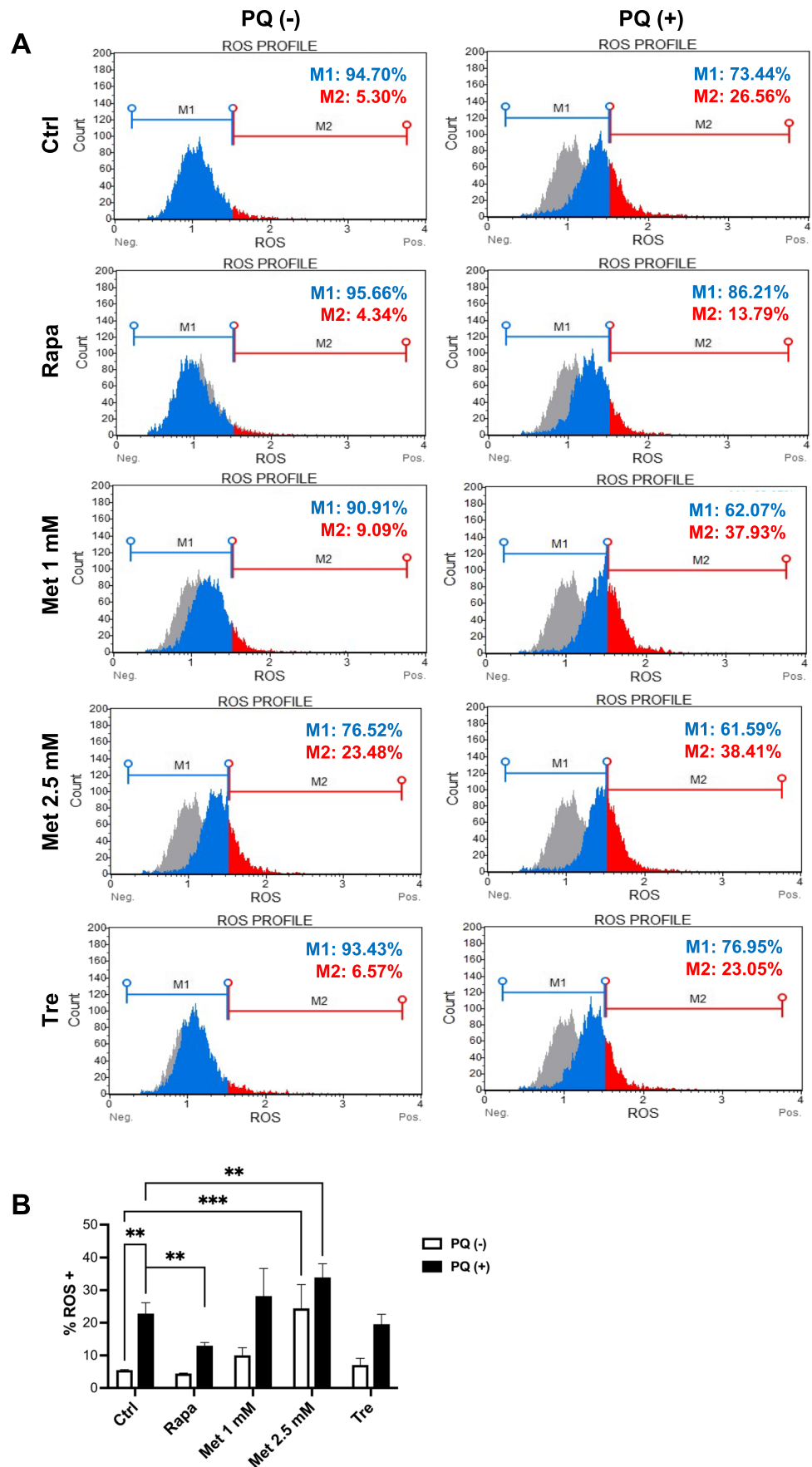
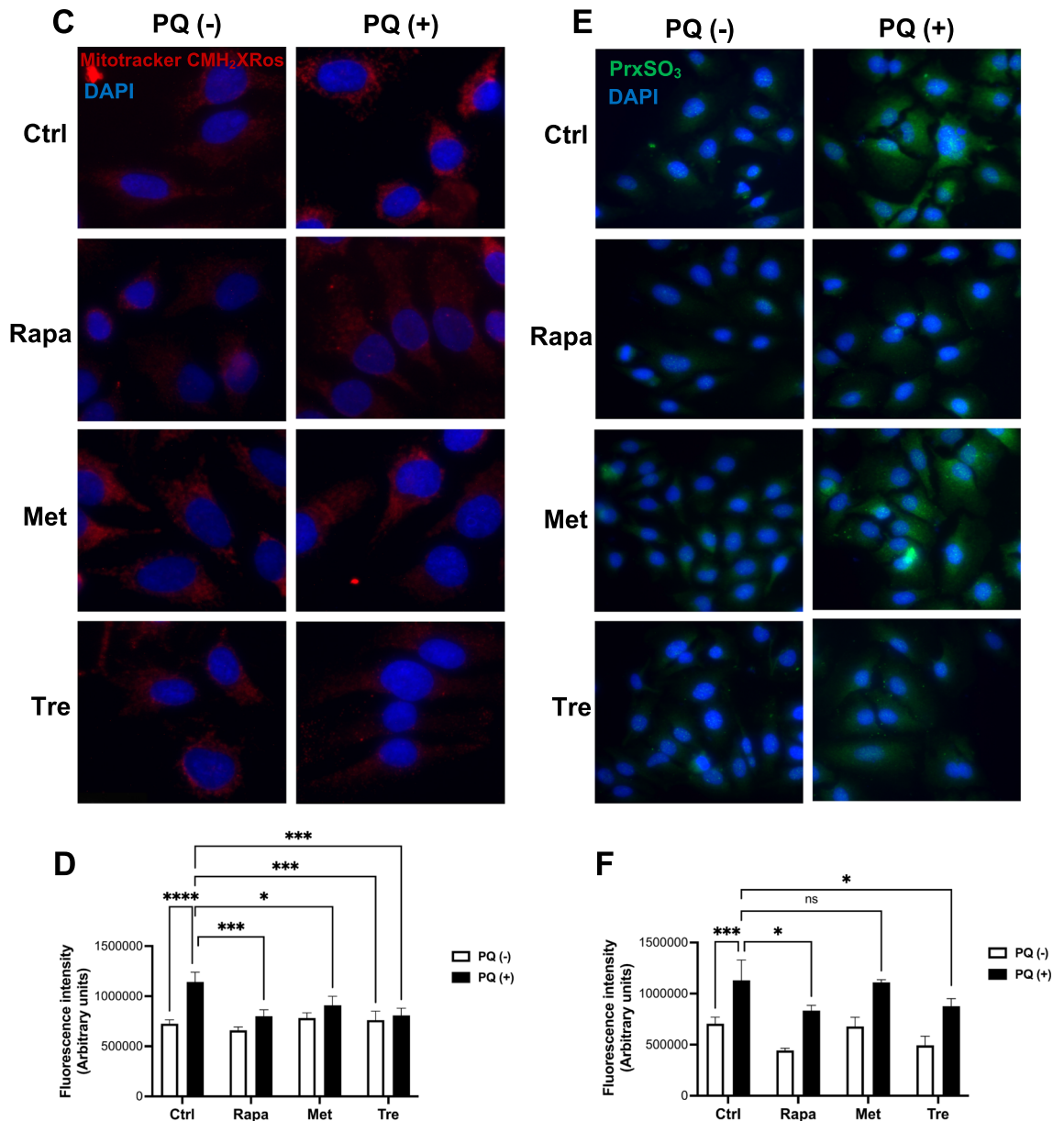


Fig. 2 (continued)



whether metformin and trehalose could also protect the cells from PQ toxicity through flow cytometry using 7-AAD and Annexin V (Fig. 3D). No statistically significant differences were detected in early apoptosis (Fig. 3E). Autophagy inducers did not affect apoptosis by themselves; while PQ caused a significant increase in the percentage of cells in late apoptosis. Interestingly, pre-treatment with metformin or trehalose prevented apoptosis induced by PQ (Fig. 3F). Viability values are shown in Supplementary Fig. 2.

Autophagy Inducers Prevent Cognitive and Motor Dysfunctions Mediated by PQ

Afterward, metformin and trehalose effect on PQ toxicity was assessed in vivo. Autophagy was stimulated 1 week before PQ treatment. Mice body weight was evaluated weekly throughout the model, and no statistically significant differences were found between groups (Supplementary Fig. 3).

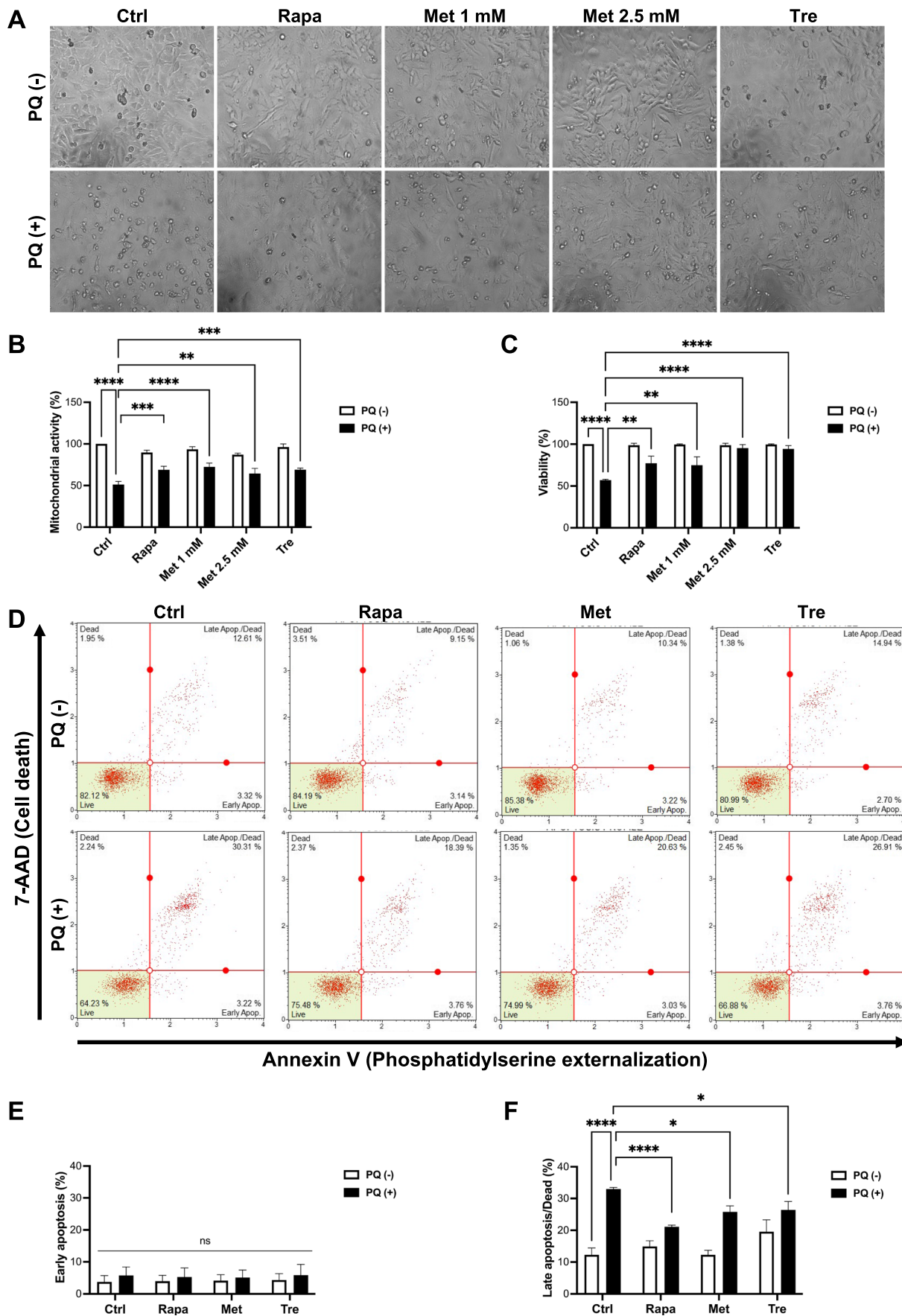


Fig. 3 Metformin and trehalose have a protective effect on mitochondrial activity and apoptosis induced by PQ. Cells were pre-treated with rapamycin (10 μ M), metformin (1 and 2.5 mM), or trehalose (100 mM) 1 h before PQ (0.5 mM) treatment, and cells were analyzed at 48 h. **A** Representative microphotographs show increased loss of adherence and floating cells in response to PQ. Cell adherence was best preserved when autophagy was induced before PQ treatment. **B** Mitochondrial activity was evaluated by MTT assay. PQ decreased mitochondrial activity compared to the control. Rapamycin, metformin, or trehalose-stimulated autophagy before PQ treatment decreased this effect. **C** Cell viability was measured by trypan blue exclusion. PQ decreased the viability percentage compared to the control, and autophagy inducers prevented its toxic effect. Statistical analysis is depicted. **D** Evaluation of apoptotic cell death by flow cytometry using annexin V and 7-AAD. **E** No significant difference was observed in the percentage of cells in early apoptosis. **F** PQ increased the percentage of late apoptosis compared to the control, and autophagy inducers reduced it. Ctrl, control; Rapa, rapamycin; Met, metformin; Tre, trehalose; PQ, paraquat. A probability value of $p < 0.05$ was considered statistically significant; * $p < 0.05$; ** $p < 0.01$; *** $p < 0.001$; **** $p < 0.0001$; ns, not significant

Cognitive impairment is among the most frequent non-motor features of PD [3]. It was evaluated through the nest-building test, which relies on the functional integrity of the sensory and motor systems, assessing behavioral integrity [46]. Furthermore, this activity requires orofacial and forelimb movement, which is dependent on dopamine [47]. Mice treated with the autophagy inducers constructed a well-organized complete dome-shaped nest similar to the control group (Fig. 4A–B). Mice treated with PQ built a disorganized cup-shaped nest. Interestingly, all autophagy inducers led to a restorative effect on the nest-building ability of mice affected by PQ.

Based on the Movement Disorder Society Clinical Diagnostic Criteria for Parkinson's disease (MDS-PD), the central character of the disease is a motor alteration [48]. Therefore, we evaluated our model's motor function using the gait test, which provides quantifiable data on movement impairments [49]. The control group showed the typical motor function, which was affected in response to PQ, evidenced by decreased hindlimbs and forelimbs stride length, while stride width was not affected (Fig. 4C–G). Autophagy stimulation prevented PQ-mediated motor alterations. So, PQ-mediated cognitive and motor disruption is prevented by all autophagy inducers.

Metformin and Trehalose Exert a Protective Effect Against Dopaminergic Neuronal Loss and Glial Cell Alteration Mediated by PQ

Since the main pathophysiological characteristic of PD is the selective loss of dopaminergic neurons in the substantia nigra [4], we evaluated whether autophagy-inducing

molecules have a protective effect on them. Mice treated with autophagy inducers showed a similar dopaminergic neurons average population as the control (Fig. 5A). A noticeable decrease in dopaminergic neurons was detected in response to PQ compared to the control. Importantly, metformin and trehalose showed a protective effect from neuronal loss induced by PQ similar to that previously reported for rapamycin [16]. These results were corroborated by tyrosine hydroxylase (TH) positive neuron count (Fig. 5E).

Oligodendrocytes wrap axons with multiple myelin sheaths to generate rapid and efficient signal transduction and provide trophic and metabolic support to neurons, promoting neuronal survival [50]. Because of oligodendrocytes' tight association with nerve fibers, we wanted to know whether these cells were affected in the PD model and protected by the autophagy inducers. Treatment with autophagy inducers does not alter the oligodendrocyte population as it remains at comparable levels to the control group. PQ caused a significant decrease in these cells population, which was prevented by pre-treatment with autophagy inducers (Fig. 5B). These findings were confirmed by quantifying the CNPase fluorescence intensity (Fig. 5F).

Astrocytes are the most abundant cell type in the CNS and actively participate in many functions like synaptic transmission control, blood flow and metabolism regulation, blood–brain barrier formation, circadian rhythms regulation, and neurogenesis [51, 52], and respond to CNS damage through a process called astrogliosis [53]. Hence, we investigated the status of astrocytes in our model. Astrocytes population remained unaltered in mice treated with the autophagy inducers compared to the control group (Fig. 5C). Mice exposed to PQ displayed an evident astrogliosis, which was avoided when autophagy was prestimulated with rapamycin, metformin, or trehalose. These data were confirmed by glial fibrillary acidic protein (GFAP) positive astrocyte count (Fig. 5G).

Microglial activation and inflammation are critical in PD pathogenesis [54]. Thus, we evaluated the effect of autophagy inducers on microglial activation mediated by PQ. The control group showed basal levels of microglial activation, which remained unaffected by autophagy stimulation (Fig. 5D). In contrast, PQ significantly increased microglial activation, and all autophagy inducers prevented it. These results were supported by ionized calcium-binding adaptor molecule 1 (IBA-1) positive microglia count (Fig. 5H).

These results indicate that autophagy stimulation prevents dopaminergic neuronal death, astrogliosis, and microgliosis induced by PQ.

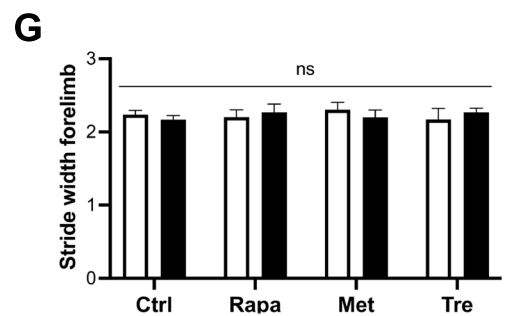
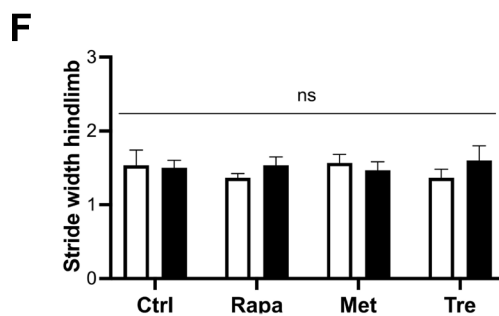
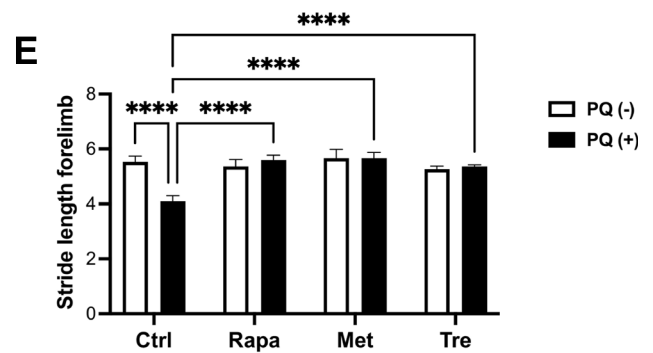
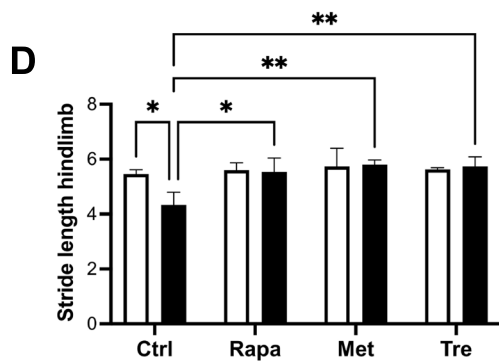
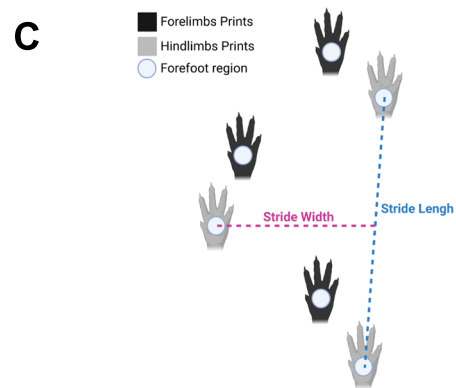
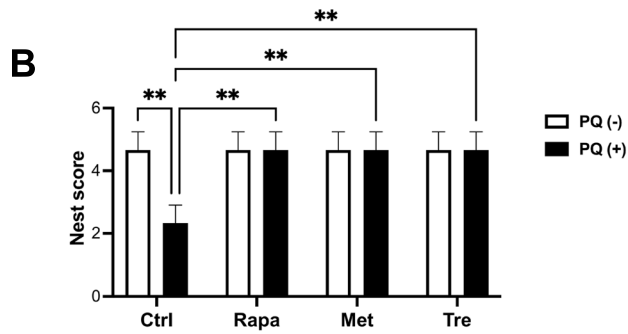
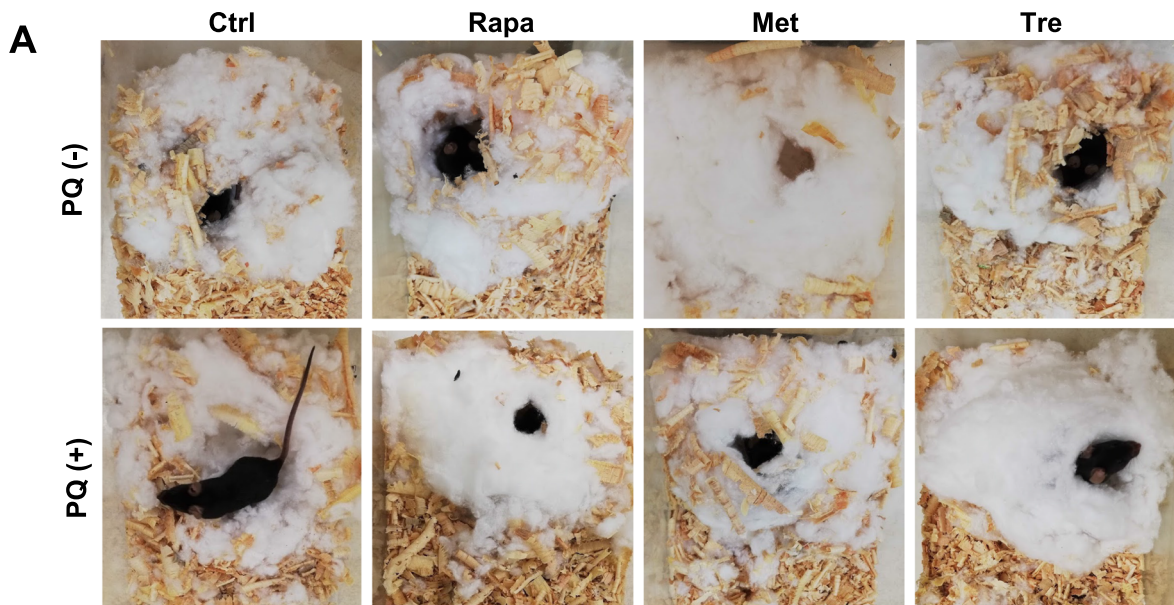


Fig. 4 Autophagy inducers metformin and trehalose prevent cognitive and motor dysfunction in the Parkinson's disease animal model. **A** Representative images of the nests built where it is shown that PQ-treated mice built nests of poor quality. In contrast, when the pre-treatment with the autophagy inducers is done, the mice build nests of higher quality. **B** The nests were scored as follows: 5 = complete dome-shaped nest, 4 = incomplete dome-shaped nest, 3 = cup-shaped nest, 2 = flat nest, 1 = disturbed, and 0 undisturbed nesting material. **C** The gait test assessed motor coordination, where the stride length and width were measured. **D** and **E** The group treated with PQ showed a shorter stride length than the control, but the mice treated with the autophagy inducers and PQ showed a similar pattern to that of the control on both hindlimbs (**D**) and forelimbs (**E**). **F** and **G** No differences were observed in the stride width on the hindlimbs (**F**) and forelimbs (**G**). Ctrl, control; Rapa, rapamycin; Met, metformin; Tre, trehalose; PQ, paraquat. A probability value of $p < 0.05$ was considered statistically significant; * $p < 0.05$; ** $p < 0.01$; **** $p < 0.0001$; ns, not significant

Autophagy Stimulation Prevents Cell Death Induced by PQ in the Substance Nigra Pars Compacta

PQ induces cell death mediated by caspase-dependent and independent apoptosis, accompanied by chromosomal DNA cleavage into fragments [55]. Therefore, we detected cell death with the TUNEL assay, which identifies DNA fragmentation based on the ability of TdT to label ends of double-stranded DNA breaks [56]. TUNEL-positive cells were dramatically increased in mice exposed to PQ, while previous stimulation with rapamycin, metformin, or trehalose abolished PQ toxicity (Fig. 6A, B).

Metformin and Trehalose Induce Autophagy Through AMPK Phosphorylation and Prevent α -Synuclein Aggregation Induced by PQ

AMP-activated protein kinase (AMPK) is a sensor of nutrients and energy, which deprivation induces autophagy via Ulk1 phosphorylation and mTOR suppression [57]. Metformin induces AMPK activation through complex 1 inhibition of the mitochondrial electron transport chain, which decreases ATP levels [58]. On the other hand, trehalose inhibits glucose transporters (GLUT), generating a glucose starvation-like state and activating autophagy through AMPK [26]. So, we evaluated AMPK phosphorylation in our model. Indeed, metformin and trehalose induced AMPK activation, which remained even when followed by PQ treatment (Fig. 7A, B). Autophagy induction by metformin and trehalose was confirmed by LC3-II detection, showing a punctuated pattern representing autophagosomes (Supplementary Fig. 4), corroborating that AMPK phosphorylation is inducing autophagy in our model.

In addition, we detected α -synuclein (α -Syn), a soluble protein highly expressed in the CNS's presynaptic terminals, and its aggregation is one of the primary PD pathophysiological features [59]. PQ-treated mice showed a punctuated

pattern depicting α -Syn aggregation (Fig. 7C). Interestingly, autophagy inducers decreased α -Syn aggregation induced by PQ (Fig. 7C, D), suggesting that autophagy induced by metformin and trehalose prevents α -Syn aggregation mediated by PQ.

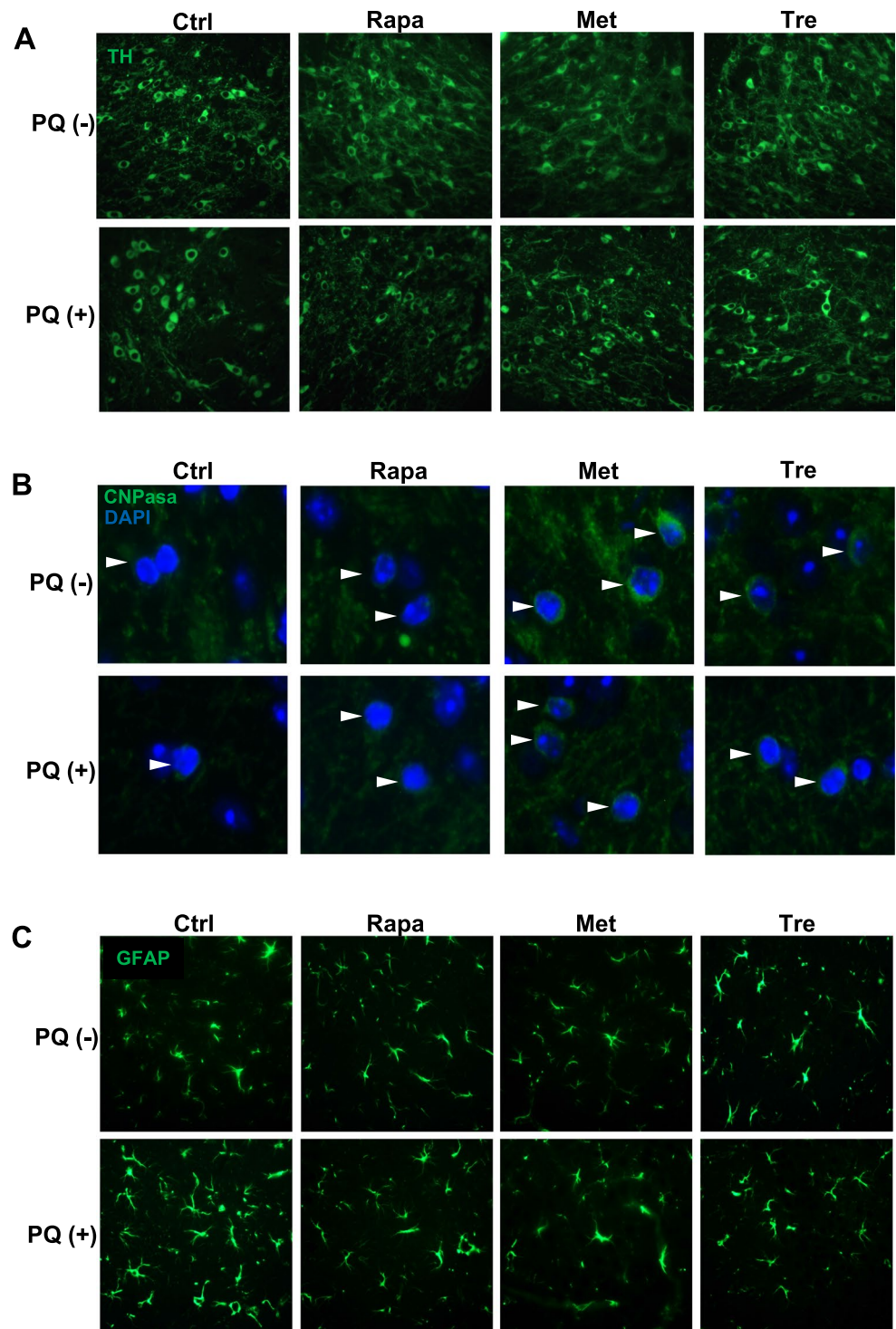
Discussion

PD is a progressive neurodegenerative disorder; unfortunately, no disease-modifying or preventative treatment is currently available. Patients with PD only have palliative treatments focused on controlling motor symptoms [60]. The current treatment for PD involves medication that mimics the dopamine effect. The most widely used medication is levodopa, combined with carbidopa, a drug that blocks levodopa conversion to dopamine outside of the CNS and thus inhibits unwanted levodopa side effects outside the CNS during PD management [61]. Therefore, searching for treatments that help to halt neuropathological alterations, such as oxidative stress, mitochondrial damage, and autophagy disruption, is essential to prevent dopaminergic neuronal death and motor symptoms that impair quality of life.

Rapamycin is the best-characterized autophagy inducer up to date and decreases both oxidative stress and dopaminergic cell death in a PQ-induced PD model [16]. Although the neuroprotective dose of rapamycin is lower than that used as an immunosuppressive agent, its neurotherapeutic application is still controversial because of its immunomodulatory properties [62]. In addition, it was recently reported that rapamycin downregulated microglial Trem2, a crucial receptor for A β plaque uptake, and decreased β -amyloid plaque removal in an Alzheimer's disease animal model, suggesting rapamycin may exacerbate A β -related pathologies [20]. Thus, it is essential to evaluate the effect of other autophagy-inducing molecules, like metformin and trehalose, in a PD model, which may exert protective effects through different mechanisms.

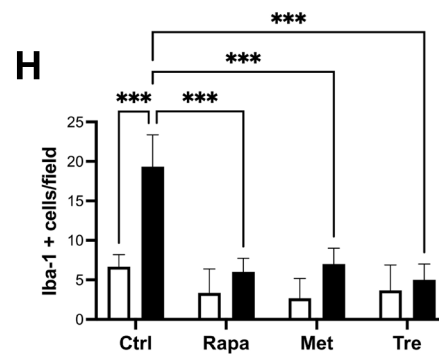
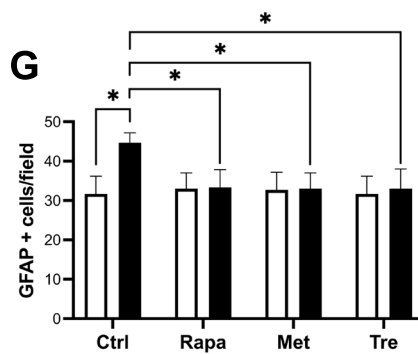
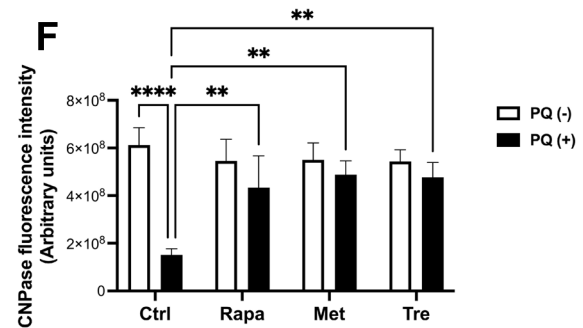
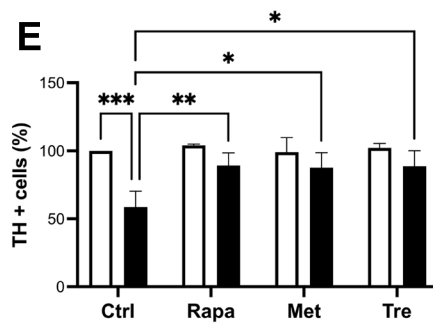
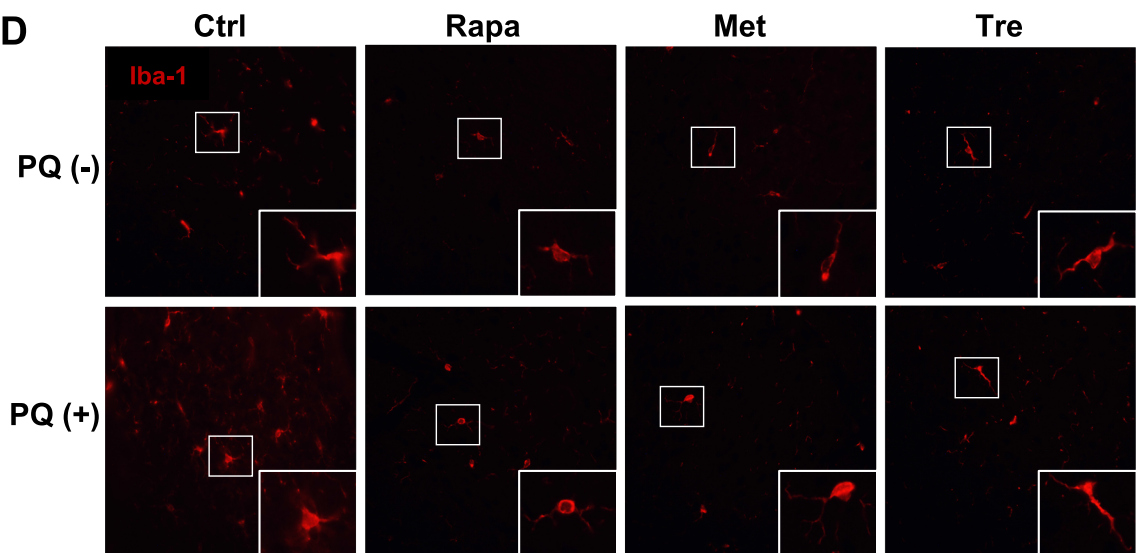
Since metformin is used for the long-term treatment of type 2 diabetes mellitus, and trehalose can be hydrolyzed into glucose, blood glucose levels could be altered during treatment with these autophagy inducers. Previous studies evaluated blood glucose levels after treatment with different trehalose concentrations, including the one used in our study (2%) [63] for 6 weeks, and even a higher concentration (5%) [64] for 13 weeks found no significant difference compared to the control group. Moreover, when metformin was administered in patients at increasing doses, from 500 to 2000 mg per day (equivalent to that used in our model) for 12 weeks, glucose tolerance and blood glucose levels were not affected [65]. However, there is a risk of alteration when used with other antidiabetic medications, intense exercise, large amounts of alcohol, or not consuming enough dietary calories [66, 67]. Therefore, the

Fig. 5 Autophagy inducers prevent dopaminergic neurons and oligodendrocytes loss, astrocytosis, and microgliosis mediated by PQ. Immunofluorescences were performed to detect **(A)** dopaminergic neurons using anti-TH antibody; **B** oligodendrocytes using anti-CNPase antibody; **C** astrocytes using anti-GFAP, and **D** activated microglia with anti-Iba-1 antibody. **E** Positive TH cell quantification. Metformin or trehalose pre-treatment protected against PQ-induced neuronal death. **F** Positive CNPase fluorescent intensity quantification. Induction of autophagy with metformin and trehalose prevents PQ-induced loss of oligodendrocytes **(G)** Positive GFAP cell quantification. PQ-induced astrocytosis was prevented by pre-treatment with autophagy inducers. **H** Quantification of Iba-1 positive fluorescence intensity. PQ caused microglia activation, resulting in neuroinflammation, which was prevented by treatment with autophagy inducers. Ctrl, control; Rapa, rapamycin; Met, metformin; Tre, trehalose; PQ, paraquat. A probability value of $p < 0.05$ was considered statistically significant; * $p < 0.05$; ** $p < 0.01$; *** $p < 0.001$; **** $p < 0.0001$



neuroprotective doses used in our study do not cause alteration in the physiological blood glucose levels, and no notable side effects have been reported. Thus, both autophagy inducers are promising candidates for PD long-term use. Furthermore, it is relevant to highlight that the metformin and trehalose doses used in our study are within the approved and recommended

doses for use in humans [68]. The metformin dose we employed corresponds to the maximum daily dose approved by the FDA (2000 mg) [68]. Regarding trehalose, the dose we used corresponds to 14.7 g per day in humans (considering an average weight of 60 kg), below the daily limit of sugar consumption recommended by the WHO, which is 25 g [69].

Fig. 5 (continued) **D**

Previously, metformin bioavailability was determined after oral administration of 150 mg/kg twice a day for 3 weeks in rats striatum (1.9 ± 0.3 nmol/g), hippocampus (7.3 ± 1 nmol/g), and CSF (44.3 ± 2.2 μ mol/L) [70]. Currently, there are no reports of trehalose bioavailability in the brain, but the enterohepatic route metabolizes about 99% of an orally ingested trehalose, and only 1% is absorbed into the bloodstream [71, 72]. Unabsorbed trehalose is likely fermented by the intestinal microbiota to short-chain fatty acids such as acetate, propionate, and butyrate [73], which raise the possibility that trehalose neuroprotective effects occur

through the microbiota-gut-brain axis [74]. Interestingly, trehalase, responsible for trehalose hydrolyzation into two glucose molecules, has been detected in mice's cerebral cortex, hippocampus, and cerebellum [75, 76], and trehalose is necessary for neuronal arborization during maturation [75].

Herein, we determined that metformin and trehalose are not toxic to dopaminergic cells and do not affect weight and survival throughout the treatments in the animal model. Metformin and trehalose have previously been reported as autophagy inducers [22, 77]. We confirmed this by detecting increased LC3-II by western blot in vitro and through

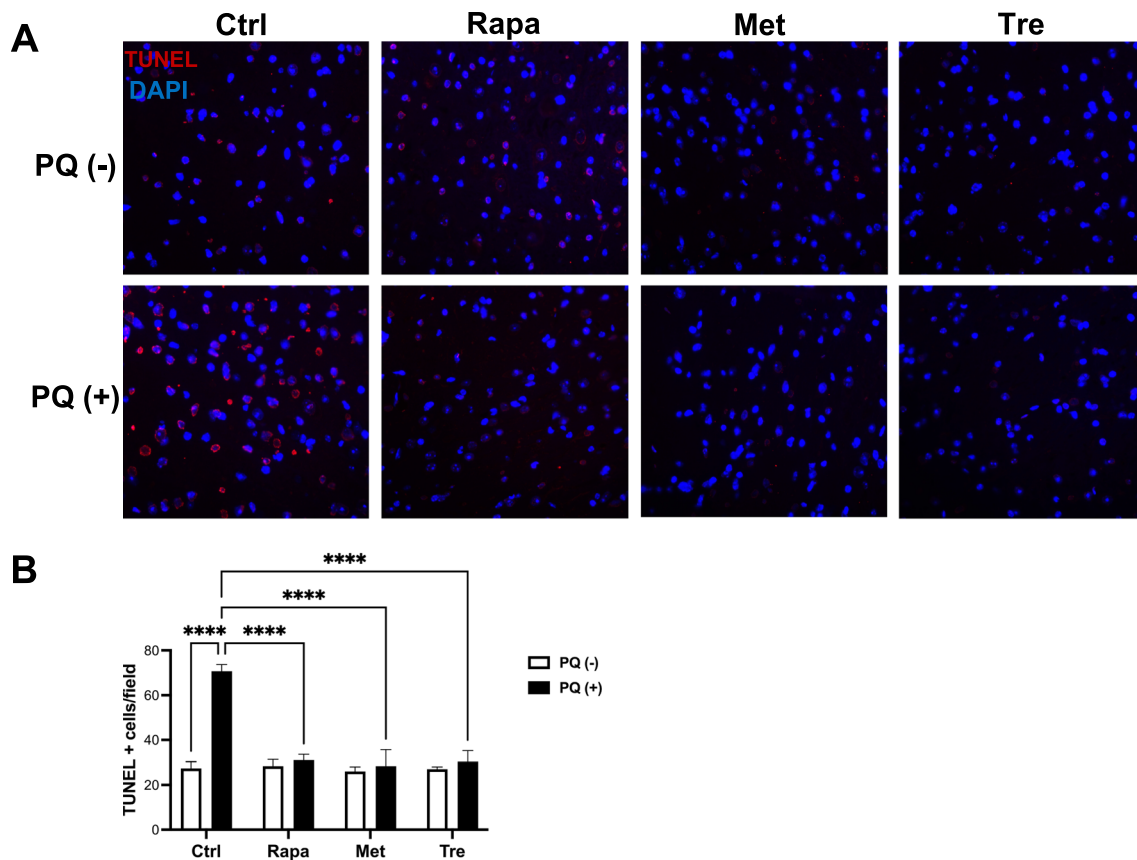


Fig. 6 Autophagy stimulated by metformin and trehalose prevents cell death induced by PQ. **A** DNA fragmentation detected by TUNEL assay. **B** TUNEL-positive cells quantification. Pre-treatment with metformin or trehalose protected from PQ-induced cell death. Ctrl,

control; Rapa, rapamycin; Met, metformin; Tre, trehalose; PQ, paraquat. A probability value of $p < 0.05$ was considered statistically significant; **** $p < 0.0001$

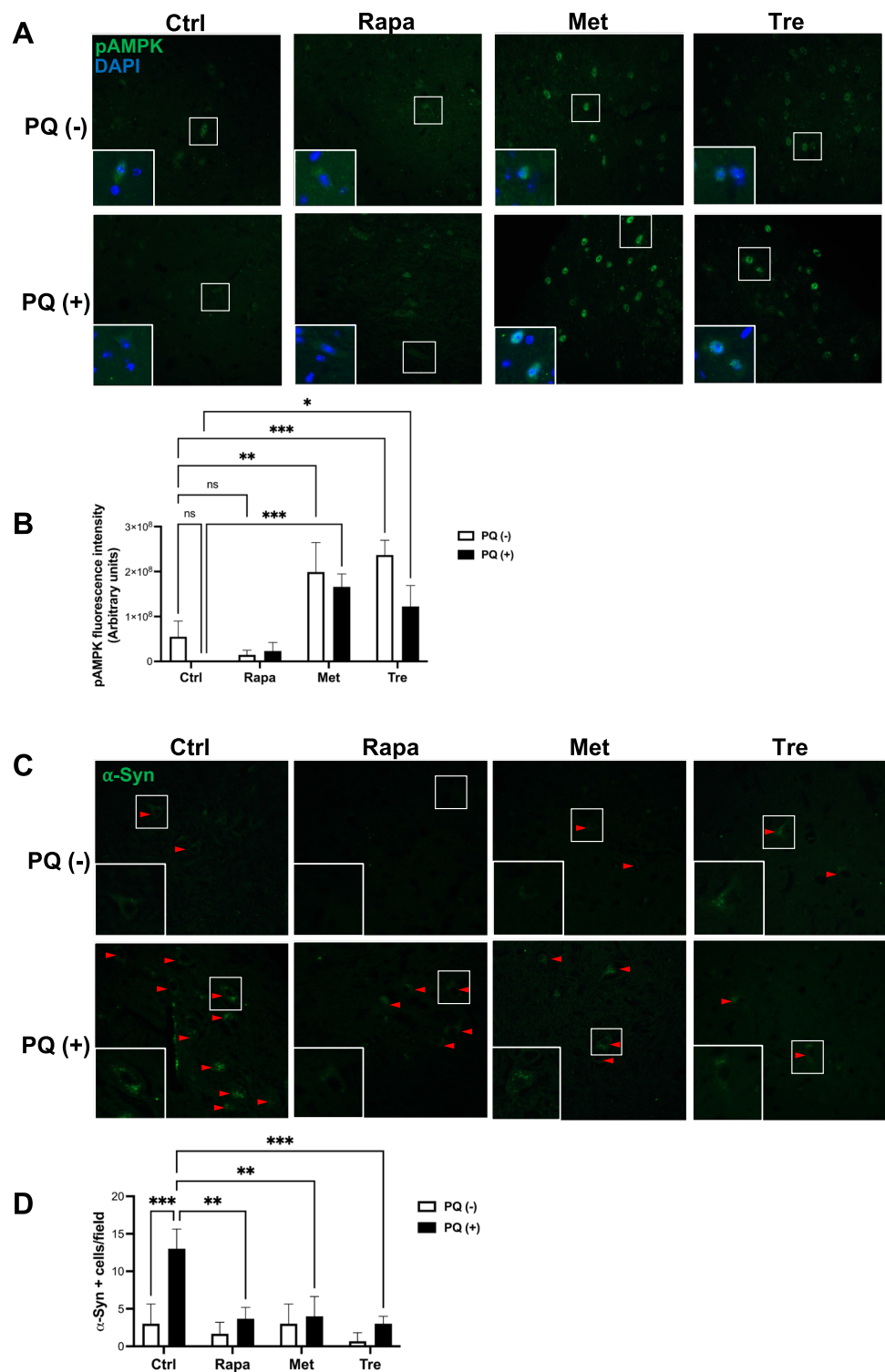
immunofluorescence *in vivo*, and autophagosomes were present in different maturation degrees (TEM) in cells treated with either of these inducers. Interestingly, also metformin and trehalose induced AMPK phosphorylation (pAMPK) at threonine 172 in the α -subunit with nuclear localization in the midbrain. Probably, pAMPK translocation to the nucleus activates autophagy by regulating the expression of genes downstream of transcription factors such as FOXO3, TFEB, and BRD4 [78]. Also, it was reported that pAMPK nuclear translocation is regulated by a nuclear localization signal, phosphorylation at threonine 172, and the starvation state induced by metformin and trehalose [24, 26, 79, 80].

Previously, we demonstrated that PQ inhibits the autophagy mechanism, which damages dopaminergic cells [8]. We demonstrated that autophagy flux inhibition and large autophagosome accumulation in response to PQ were prevented by inducing autophagy with metformin or trehalose, reestablishing autophagy flux. It was consistent with LC3-II decrease in PQ-treated cells and increased level when autophagy was prestimulated. These findings correlate with

the effect of rapamycin-induced autophagy in the PD model induced with PQ [16].

Autophagy promotes neuron survival by degrading and recycling intracellular content under unfavorable conditions for cells, including oxidative stress [81]. When autophagy was stimulated with metformin or trehalose in the PQ-induced PD model, there was no antioxidant effect on ROS in the cytoplasm but an antioxidant effect in mitochondria. These results may be because the mitochondria are the main target of PQ and the compartment where oxidative stress begins [43, 82]. In addition, we observed a decrease in the Prxs hyperoxidation mediated by PQ in response to trehalose. This finding concurs with other studies, where both autophagy inducers decreased oxidative stress [83, 84]. When autophagy was induced with metformin (1 mM and 2.5 mM) in the PD model, increased ROS levels in the cytoplasm were observed. In addition, metformin, at 2.5 mM, increased the basal oxidative stress, which can be explained because metformin inhibits mGPDH, preventing electrons from cytosolic NADH (formed during glycolysis) from being transported

Fig. 7 Metformin and trehalose induce autophagy through AMPK phosphorylation and prevent α -synuclein aggregation. **A** AMPK phosphorylation (pAMPK) was assessed with anti-pAMPK, and **(B)** its fluorescence intensity was quantified. Metformin and trehalose induced AMPK phosphorylation and translocation to the nuclear compartment, indicating its activation and, therefore, the induction of autophagy. **C** Detection of α -Syn by immunofluorescence, and **(D)** quantification of α -Syn positive cells. Pre-treatment with the autophagy inducers protected from PQ-induced protein aggregation. Ctrl, control; Rapa, rapamycin; Met, metformin; Tre, trehalose; PQ, paraquat. A probability value of $p < 0.05$ was considered statistically significant; * $p < 0.05$; ** $p < 0.01$; *** $p < 0.001$; ns, not significant



to mitochondria to be oxidized to NAD^+ , resulting in increased cytoplasmic oxidation and decreased mitochondrial oxidation [23, 24].

When evaluating the effect of metformin and trehalose on the toxicity induced by PQ, an increase in mitochondrial activity and viability was observed, indicating

a protective effect of autophagy stimulation. Our PD animal model induced with PQ exhibited cognitive and gait pattern alterations related to PD patients' phenotype (3). Pre-treatment with metformin or trehalose prevented cognitive and motor dysfunctions. Additionally, both autophagy inducers decreased dopaminergic neuronal loss and DNA

fragmentation mediated by PQ to levels comparable to the control group, suggesting a protective effect. These findings agree with the neuroprotective effect of metformin on dopaminergic neurons in a mice PD model induced with MPTP/P [83]. Also, trehalose showed a neuroprotective effect in a tauopathy mice model with parkinsonism, overexpressing the parkin-deletion-mutated human tau protein (PK(-/-)/Tau(VLW)) [85].

Moreover, prestimulation with metformin or trehalose prevented oligodendrocytes loss, astrogliosis, microgliosis, and α -synuclein aggregation induced by PQ. Notably, demyelination and oligodendrocyte dysfunction have been associated with PD, where the myelination degree is a crucial factor determining the neurons' vulnerability to α -Syn aggregation [86]. Indeed α -Syn accumulation was higher in demyelinated axons in postmortem studies in PD patients [87], which concurs with the effect of PQ in our study. Importantly, pre-treatment with metformin or trehalose protects against the loss of oligodendrocytes, which is associated with the prevention of α -Syn aggregation and dopaminergic neuronal loss. Besides, astrocytes respond to CNS damage through a process called astrogliosis, which may occur in response to PQ-induced oxidative stress. Astrocytes overexpressed Nrf2 to regulate antioxidant enzymes transcriptionally, having a higher antioxidant potential than neurons [88, 89], which is consistent with oxidative stress controlled by metformin and trehalose and subsequently decreased astrogliosis. Based on postmortem samples and neuroimaging analysis, microglia and α -synuclein aggregation are involved in PD pathophysiology, which agrees with our findings, and both are prevented by autophagy inducers [90, 91].

Conclusions

In this study, the neuroprotective potential of metformin and trehalose was evaluated comparatively for the first time in a PD model of epidemiologic relevance. In summary, we demonstrated that both autophagy inducers, metformin, and trehalose, showed an antioxidant effect, improved mitochondrial activity, and decreased dopaminergic cell death induced by PQ *in vitro*. Also, cognitive and motor deteriorated functions, dopaminergic neurons and oligodendrocytes loss, astrogliosis, microgliosis, and cell death mediated by PQ were prevented by both autophagy inducers *in vivo*. Finally, metformin and trehalose induced autophagy through AMPK phosphorylation (pAMPK) and decreased α -synuclein accumulation. Therefore, metformin and trehalose are promising neurotherapeutic autophagy inducers with great potential for treating neurodegenerative diseases such as PD. Hence in the near future, these molecules may provide different low-cost therapeutic alternatives for patients with PD.

Supplementary Information The online version contains supplementary material available at <https://doi.org/10.1007/s12035-023-03530-5>.

Acknowledgements YGC (No. CVU: 856246) received a scholarship from Consejo Nacional de Ciencia y Tecnología (CONACYT). The graphical abstract were created with Biorender.com.

Authors Contribution AGG and HRR conceived, designed, and analyzed the experiments. YGC performed all the experiments, statistical analysis, and interpretation of data. OSC, MJLA, and RMOL analyzed the data, revised and provided feedback on the manuscript. YGC and AGG wrote the paper. All the authors reviewed and approved the final version of the manuscript.

Funding This work received support from Programa de Apoyo a la Investigación Científica y Tecnológica (PAICYT): SA1872-21 and 254-CS-2022 (AGG).

Data Availability The datasets generated during and/or analysed during the current study are available in the manuscript.

Declarations

Ethics Approval All experiments were conducted under the Mexican Official Norm "NOM-062-ZOO-1999" (De Aluja, 2002) and the Institutional Committee for the Care and Use of Laboratory Animals (Comite Institucional para el Cuidado y Uso de los Animales de Laboratorio, CICUAL), and approved by the Ethical Committee of Facultad de Medicina de Universidad Autónoma de Nuevo Leon on June 14, 2019 (registration number HT19-00002).

Consent to Participate Not applicable.

Consent for Publication Not applicable.

Conflict of Interest The authors declare no conflict of interest.

References

1. WHO Global Health Estimates (2023) Life expectancy and leading causes of death and disability. World Health Organization. <https://www.who.int/data/gho/data/themes/mortality-and-global-health-estimates/gho-life-expectancy-and-healthy-life-expectancy>. Accessed 18 Feb 2023
2. Giacomello E, Toniolo L (2021) Nutrition, diet and healthy aging. *Nutrients* 14(1). <https://doi.org/10.3390/nu14010190>
3. Kalia LV, Lang AE (2015) Parkinson's disease. *Lancet* 386(9996):896–912. [https://doi.org/10.1016/S0140-6736\(14\)61393-3](https://doi.org/10.1016/S0140-6736(14)61393-3)
4. Dickson DW (2018) Neuropathology of Parkinson disease. *Parkinsonism Relat Disord* 46(Suppl 1):S30–S33. <https://doi.org/10.1016/j.parkreldis.2017.07.033>
5. Tanner CM, Kamel F, Ross GW, Hoppin JA, Goldman SM, Korell M, Marras C, Bhudhikanok GS, Kasten M, Chade AR, Comyns K, Richards MB, Meng C, Priestley B, Fernandez HH, Cambi F, Umbach DM, Blair A, Sandler DP, Langston JW (2011) Rotenone, paraquat, and Parkinson's disease. *Environ Health Perspect* 119(6):866–872. <https://doi.org/10.1289/ehp.1002839>
6. Nisticò R, Mehdawy B, Piccirilli S, Mercuri N (2011) Paraquat- and rotenone-induced models of Parkinson's disease. *Int J Immunopathol Pharmacol* 24(2):313–322. <https://doi.org/10.1177/039463201102400205>

7. Powers R, Lei S, Anandhan A, Marshall DD, Worley B, Cerny RL, Dodds ED, Huang Y, Panayiotidis MI, Pappa A, Franco R (2017) Metabolic investigations of the molecular mechanisms associated with parkinson's disease. *Metabolites* 7(2). <https://doi.org/10.3390/metabo7020022>
8. Garcia-Garcia A, Anandhan A, Burns M, Chen H, Zhou Y, Franco R (2013) Impairment of Atg5-dependent autophagic flux promotes paraquat- and MPP+-induced apoptosis but not rotenone or 6-hydroxydopamine toxicity. *Toxicol Sci*. <https://doi.org/10.1093/toxsci/kft188>
9. Do J, McKinney C, Sharma P, Sidransky E (2019) Glucocerebrosidase and its relevance to parkinson disease. *Mol Neurodegener* 14(1):36. <https://doi.org/10.1186/s13024-019-0336-2>
10. Anglade P, Vyas S, Javoy-Agid F, Herrero MT, Michel PP, Marquez J, Mouatt-Prigent A, Ruberg M, Hirsch EC, Agid Y (1997) Apoptosis and autophagy in nigral neurons of patients with Parkinson's disease. *Histol Histopathol* 12(1):25–31
11. Gómez-Virgilio L, Silva-Lucero MD, Flores-Morelos DS, Gallardo-Nieto J, Lopez-Toledo G, Abarca-Fernandez AM, Zacapala-Gómez AE, Luna-Muñoz J, Montiel-Sosa F, Soto-Rojas LO, Pacheco-Herrero M, Cardenas-Aguayo MD (2022) Autophagy: a key regulator of homeostasis and disease: an overview of molecular mechanisms and modulators. *Cells* 11(15). <https://doi.org/10.3390/cells11152262>
12. Komatsu M, Waguri S, Chiba T, Murata S, Iwata J, Tanida I, Ueno T, Koike M, Uchiyama Y, Kominami E, Tanaka K (2006) Loss of autophagy in the central nervous system causes neurodegeneration in mice. *Nature* 441(7095):880–884. <https://doi.org/10.1038/nature04723>
13. Hara T, Nakamura K, Matsui M, Yamamoto A, Nakahara Y, Suzuki-Migishima R, Yokoyama M, Mishima K, Saito I, Okano H, Mizushima N (2006) Suppression of basal autophagy in neural cells causes neurodegenerative disease in mice. *Nature* 441(7095):885–889. <https://doi.org/10.1038/nature04724>
14. Erekat NS (2022) Autophagy and its association with genetic mutations in parkinson disease. *Med Sci Monit* 28:e938519. <https://doi.org/10.12659/MSM.938519>
15. Lizama BN, Chu CT (2021) Neuronal autophagy and mitophagy in Parkinson's disease. *Mol Aspects Med* 82:100972. <https://doi.org/10.1016/j.mam.2021.100972>
16. Ramirez-Moreno MJ, Duarte-Jurado APG-C, Gonzalez-Alcocer Y, Alfredo L-A-C, Montes-de-Oca-Luna O, Rodriguez-Rocha R, Humberto G-G (2019) Autophagy stimulation decreases dopaminergic neuronal death mediated by oxidative stress. *Mol Neurobiol*. <https://doi.org/10.1007/s12035-019-01654-1>
17. Rowinsky EK (2004) Targeting the molecular target of rapamycin (mTOR). *Curr Opin Oncol* 16(6):564–575. <https://doi.org/10.1097/01.cco.0000143964.74936.d1>
18. Fleming A, Noda T, Yoshimori T, Rubinsztein DC (2011) Chemical modulators of autophagy as biological probes and potential therapeutics. *Nat Chem Biol* 7(1):9–17. <https://doi.org/10.1038/nchembio.500>
19. Harris H, Rubinsztein DC (2011) Control of autophagy as a therapy for neurodegenerative disease. *Nat Rev Neurol* 8(2):108–117. <https://doi.org/10.1038/nrneuro.2011.200>
20. Shi Q, Chang C, Saliba A, Bhat MA (2022) Microglial mtor activation upregulates Trem2 and enhances β -amyloid plaque clearance in the in the 5XFAD alzheimer's disease model. *J Neurosci* 42(27):5294–5313. <https://doi.org/10.1523/JNEUROSCI.2427-21.2022>
21. Sanchez-Rangel E, Inzucchi SE (2017) Metformin: clinical use in type 2 diabetes. *Diabetologia* 60(9):1586–1593. <https://doi.org/10.1007/s00125-017-4336-x>
22. Thellung S, Corsaro A, Nizzari M, Barbieri F, Florio T (2019) Autophagy activator drugs: a new opportunity in neuroprotection from misfolded protein toxicity. *Int J Mol Sci* 20(4). <https://doi.org/10.3390/ijms20040901>
23. Vial G, Detaille D, Guigas B (2019) Role of mitochondria in the mechanism(s) of action of metformin. *Front Endocrinol (Lausanne)* 10:294. <https://doi.org/10.3389/fendo.2019.00294>
24. Madiraju AK, Erion DM, Rahimi Y, Zhang XM, Braddock DT, Albright RA, Prigaro BJ, Wood JL, Bhanot S, MacDonald MJ, Jurczak MJ, Camporez JP, Lee HY, Cline GW, Samuel VT, Kibbey RG, Shulman GI (2014) Metformin suppresses gluconeogenesis by inhibiting mitochondrial glycerophosphate dehydrogenase. *Nature* 510(7506):542–546. <https://doi.org/10.1038/nature13270>
25. Sarkar S, Davies JE, Huang Z, Tunnacliffe A, Rubinsztein DC (2007) Trehalose, a novel mTOR-independent autophagy enhancer, accelerates the clearance of mutant huntingtin and alpha-synuclein. *J Biol Chem* 282(8):5641–5652. M609532200 [pii] <https://doi.org/10.1074/jbc.M609532200>
26. Mardones P, Rubinsztein DC, Hetz C (2016) Mystery solved: Trehalose kickstarts autophagy by blocking glucose transport. *Sci Signal* 9(416):fs2. <https://doi.org/10.1126/scisignal.aaf1937>
27. Rusmini P, Cortese K, Crippa V, Cristofani R, Cicardi ME, Ferrari V, Vezzoli G, Tedesco B, Meroni M, Messi E, Piccolella M, Galbiati M, Garrè M, Morelli E, Vaccari T, Poletti A (2019) Trehalose induces autophagy via lysosomal-mediated TFEB activation in models of motoneuron degeneration. *Autophagy* 15(4):631–651. <https://doi.org/10.1080/15548627.2018.1535292>
28. Byun S, Lee E, Lee KW (2017) Therapeutic implications of autophagy inducers in immunological disorders, infection, and cancer. *Int J Mol Sci* 18(9). <https://doi.org/10.3390/ijms18091959>
29. Vidal RL, Matus S, Bargsted L, Hetz C (2014) Targeting autophagy in neurodegenerative diseases. *Trends Pharmacol Sci* 35(11):583–591. <https://doi.org/10.1016/j.tips.2014.09.002>
30. Russo M, Russo GL (2018) Autophagy inducers in cancer. *Biochem Pharmacol* 153:51–61. <https://doi.org/10.1016/j.bcp.2018.02.007>
31. Gaskill BN, Karas AZ, Garner JP, Pritchett-Corning KR (2013) Nest building as an indicator of health and welfare in laboratory mice. *J Vis Exp* 82:51012. <https://doi.org/10.3791/51012>
32. Wertman V, Gromova A, La Spada AR, Cortes CJ (2019) Low-cost gait analysis for behavioral phenotyping of mouse models of neuromuscular disease. *J Vis Exp* (149). <https://doi.org/10.3791/59878>
33. Alam ZI, Daniel SE, Lees AJ, Marsden DC, Jenner P, Halliwell B (1997) A generalised increase in protein carbonyls in the brain in Parkinson's but not incidental Lewy body disease. *J Neurochem* 69(3):1326–1329
34. Alam ZI, Jenner A, Daniel SE, Lees AJ, Cairns N, Marsden CD, Jenner P, Halliwell B (1997) Oxidative DNA damage in the parkinsonian brain: an apparent selective increase in 8-hydroxyguanine levels in substantia nigra. *J Neurochem* 69(3):1196–1203
35. Dexter DT, Carter CJ, Wells FR, Javoy-Agid F, Agid Y, Lees A, Jenner P, Marsden CD (1989) Basal lipid peroxidation in substantia nigra is increased in Parkinson's disease. *J Neurochem* 52(2):381–389
36. Henchcliffe C, Beal MF (2008) Mitochondrial biology and oxidative stress in Parkinson disease pathogenesis. *Nat Clin Pract Neurol* 4(11):600–609. ncpneuro0924 [pii]. <https://doi.org/10.1038/ncpneuro0924>
37. Schapira AH (2008) Mitochondria in the aetiology and pathogenesis of Parkinson's disease. *Lancet Neurol* 7(1):97–109. S1474–4422(07)70327–7 [pii]. [https://doi.org/10.1016/S1474-4422\(07\)70327-7](https://doi.org/10.1016/S1474-4422(07)70327-7)
38. Ramirez-Moreno MJ, Duarte-Jurado AP, Gopar-Cuevas Y, Gonzalez-Alcocer A, Loera-Arias MJ, Saucedo-Cardenas O, Montes de Oca-Luna R, Rodriguez-Rocha H, Garcia-Garcia A (2019) Autophagy stimulation decreases dopaminergic neuronal death mediated by oxidative stress. *Mol Neurobiol*. <https://doi.org/10.1007/s12035-019-01654-1>
39. Singh A, Kukreti R, Saso L, Kukreti S (2019) Oxidative stress: a key modulator in neurodegenerative diseases. *Molecules* 24(8). <https://doi.org/10.3390/molecules24081583>

40. Karplus PA (2015) A primer on peroxiredoxin biochemistry. *Free Radic Biol Med* 80:183–190. <https://doi.org/10.1016/j.freeradbiomed.2014.10.009>
41. Collins JA, Wood ST, Nelson KJ, Rowe MA, Carlson CS, Chubinskaya S, Poole LB, Furdul CM, Loeser RF (2016) oxidative stress promotes peroxiredoxin hyperoxidation and attenuates pro-survival signaling in aging chondrocytes. *J Biol Chem* 291(13):6641–6654. <https://doi.org/10.1074/jbc.M115.693523>
42. Hornykiewicz O (2006) The discovery of dopamine deficiency in the parkinsonian brain. *J Neural Transm Suppl* 70:9–15. https://doi.org/10.1007/978-3-211-45295-0_3
43. Rodriguez-Rocha H, Garcia-Garcia A, Pickett C, Li S, Jones J, Chen H, Webb B, Choi J, Zhou Y, Zimmerman MC, Franco R (2013) Compartmentalized oxidative stress in dopaminergic cell death induced by pesticides and complex I inhibitors: Distinct roles of superoxide anion and superoxide dismutases. *Free Radic Biol Med* 61C:370–383. <https://doi.org/10.1016/j.freeradbiomed.2013.04.021>
44. Gray JP, Heck DE, Mishin V, Smith PJ, Hong JY, Thiruchelvam M, Cory-Slechta DA, Laskin DL, Laskin JD (2007) Paraquat increases cyanide-insensitive respiration in murine lung epithelial cells by activating an NAD(P)H:paraquat oxidoreductase: identification of the enzyme as thioredoxin reductase. *J Biol Chem* 282(11):7939–7949. <https://doi.org/10.1074/jbc.M611817200>
45. Fei Q, McCormack AL, Di Monte DA, Ethell DW (2008) Paraquat neurotoxicity is mediated by a Bak-dependent mechanism. *J Biol Chem* 283(6):3357–3364. <https://doi.org/10.1074/jbc.M708451200>
46. Kraeuter AK, Guest PC, Sarnyai Z (2019) The nest building test in mice for assessment of general well-being. *Methods Mol Biol* 1916:87–91. https://doi.org/10.1007/978-1-4939-8994-2_7
47. Sager TN, Kirchhoff J, Mørk A, Van Beek J, Thirstrup K, Didriksen M, Lauridsen JB (2010) Nest building performance following MPTP toxicity in mice. *Behav Brain Res* 208(2):444–449. <https://doi.org/10.1016/j.bbr.2009.12.014>
48. Postuma RB, Berg D, Stern M, Poewe W, Olanow CW, Oertel W, Obeso J, Marek K, Litvan I, Lang AE, Halliday G, Goetz CG, Gasser T, Dubois B, Chan P, Bloem BR, Adler CH, Deuschl G (2015) MDS clinical diagnostic criteria for Parkinson's disease. *Mov Disord* 30(12):1591–1601. <https://doi.org/10.1002/mds.26424>
49. Carter RJ, Morton J, Dunnett SB (2001) Motor coordination and balance in rodents. *Curr Protoc Neurosci Chapter 8:Unit 8.12*. <https://doi.org/10.1002/0471142301.ns0812s15>
50. Baumann N, Pham-Dinh D (2001) Biology of oligodendrocyte and myelin in the mammalian central nervous system. *Physiol Rev* 81(2):871–927. <https://doi.org/10.1152/physrev.2001.81.2.871>
51. Guillamón-Vivancos T, Gómez-Pinedo U, Matías-Guiu J (2015) Astrocytes in neurodegenerative diseases (I): function and molecular description. *Neurologia* 30(2):119–129. <https://doi.org/10.1016/j.nrl.2012.12.007>
52. Freeman MR (2010) Specification and morphogenesis of astrocytes. *Science* 330(6005):774–778. <https://doi.org/10.1126/science.1190928>
53. Sofroniew MV (2014) Astroglialosis. *Cold Spring Harb Perspect Biol* 7(2):a020420. <https://doi.org/10.1101/cshperspect.a020420>
54. Ho MS (2019) Microglia in Parkinson's disease. *Adv Exp Med Biol* 1175:335–353. https://doi.org/10.1007/978-981-13-9913-8_13
55. Zhang JH, Xu M (2000) DNA fragmentation in apoptosis. *Cell Res* 10(3):205–211. <https://doi.org/10.1038/sj.cr.7290049>
56. Kyrylkova K, Kyryachenko S, Leid M, Kiousi C (2012) Detection of apoptosis by TUNEL assay. *Methods Mol Biol* 887:41–47. https://doi.org/10.1007/978-1-61779-860-3_5
57. Kim J, Kundu M, Viollet B, Guan KL (2011) AMPK and mTOR regulate autophagy through direct phosphorylation of Ulk1. *Nat Cell Biol* 13(2):132–141. <https://doi.org/10.1038/ncb2152>
58. Foretz M, Guigas B, Bertrand L, Pollak M, Viollet B (2014) Metformin: from mechanisms of action to therapies. *Cell Metab* 20(6):953–966. <https://doi.org/10.1016/j.cmet.2014.09.018>
59. Recchia A, Debetto P, Negro A, Guidolin D, Skaper SD, Giusti P (2004) Alpha-synuclein and Parkinson's disease. *FASEB J* 18(6):617–626. <https://doi.org/10.1096/fj.03-0338rev>
60. Ng JSC (2018) Palliative care for Parkinson's disease. *Ann Palliat Med* 7(3):296–303. <https://doi.org/10.21037/apm.2017.12.02>
61. Reich SG, Savitt JM (2019) Parkinson's disease. *Med Clin North Am* 103(2):337–350. <https://doi.org/10.1016/j.mcna.2018.10.014>
62. Gonzalez-Alcocer A, Gopar-Cuevas Y, Soto-Dominguez A, Loera-Arias MJ, Saucedo-Cardenas O, Montes de Oca-Luna R, Rodriguez-Rocha H, Garcia-Garcia A (2022) Peripheral tissular analysis of rapamycin's effect as a neuroprotective agent in vivo. *Naunyn Schmiedebergs Arch Pharmacol* 395(10):1239–1255. <https://doi.org/10.1007/s00210-022-02276-6>
63. He Q, Koprach JB, Wang Y, Yu WB, Xiao BG, Brotchie JM, Wang J (2016) Treatment with trehalose prevents behavioral and neurochemical deficits produced in an AAV α -synuclein rat model of Parkinson's disease. *Mol Neurobiol* 53(4):2258–2268. <https://doi.org/10.1007/s12035-015-9173-7>
64. Perucho J, Casarejos MJ, Gomez A, Solano RM, de Yébenes JG, Mena MA (2012) Trehalose protects from aggravation of amyloid pathology induced by isoflurane anesthesia in APP(swe) mutant mice. *Curr Alzheimer Res* 9(3):334–343. <https://doi.org/10.2174/156720512800107573>
65. Carlsen SM, Grill V, Følling I (1998) Evidence for dissociation of insulin- and weight-reducing effects of metformin in non-diabetic male patients with coronary heart disease. *Diabetes Res Clin Pract* 39(1):47–54. [https://doi.org/10.1016/s0168-8227\(97\)00121-6](https://doi.org/10.1016/s0168-8227(97)00121-6)
66. Nasri H, Rafieian-Kopaei M (2014) Metformin: current knowledge. *J Res Med Sci* 19(7):658–664
67. Harada N (2020) Effects of metformin on blood glucose levels and bodyweight mediated through intestinal effects. *J Diabetes Investig* 11(6):1420–1421. <https://doi.org/10.1111/jdi.13301>
68. FDA GLUCOPHAGE® XR (2000) Metformin hydrochloride extended-released tablets. Food Drug and Administration. https://www.accessdata.fda.gov/drugsatfda_docs/label/2000/212021bl.pdf. Accessed 21 Mar 2023
69. WHO (2023) Opens public consultation on draft sugars guideline. World Health Organization. <https://www.who.int/news/item/05-03-2014-who-opens-public-consultation-on-draft-sugars-guideline>. Accessed 18 Feb 2023
70. Łabuzek K, Suchy D, Gabryel B, Bielecka A, Liber S, Okopień B (2010) Quantification of metformin by the HPLC method in brain regions, cerebrospinal fluid and plasma of rats treated with lipopolysaccharide. *Pharmacol Rep* 62(5):956–965. [https://doi.org/10.1016/s1734-1140\(10\)70357-1](https://doi.org/10.1016/s1734-1140(10)70357-1)
71. Zhang Y, DeBosch BJ (2019) Using trehalose to prevent and treat metabolic function: effectiveness and mechanisms. *Curr Opin Clin Nutr Metab Care* 22(4):303–310. <https://doi.org/10.1097/MCO.0000000000000568>
72. Jeong SJ, Stitham J, Evans TD, Zhang X, Rodriguez-Velez A, Yeh YS, Tao J, Takabatake K, Epelman S, Lodhi JJ, Schilling JD, DeBosch BJ, Diwan A, Razani B (2021) Trehalose causes low-grade lysosomal stress to activate TFEB and the autophagy-lysosome biogenesis response. *Autophagy* 17(11):3740–3752. <https://doi.org/10.1080/1548627.2021.1896906>
73. Stachowicz A, Wiśniewska A, Kuś K, Kiepusa A, Gębska A, Gajda M, Białaś M, Totoń-Żurańska J, Stachyra K, Suski M, Jawień J, Korbust R, Olszanecki R (2019) The influence of trehalose on atherosclerosis and hepatic steatosis in apolipoprotein E knockout mice. *Int J Mol Sci* 20(7). <https://doi.org/10.3390/ijms20071552>
74. Lee HJ, Yoon YS, Lee SJ (2018) Mechanism of neuroprotection by trehalose: controversy surrounding autophagy induction. *Cell Death Dis* 9(7):712. <https://doi.org/10.1038/s41419-018-0749-9>
75. Martano G, Gerosa L, Prada I, Garrone G, Krogh V, Verderio C, Passafaro M (2017) Biosynthesis of astrocytic trehalose regulates

- neuronal arborization in hippocampal neurons. *ACS Chem Neurosci* 8(9):1865–1872. <https://doi.org/10.1021/acchemneuro.7b00177>
76. Halbe L, Rami A (2019) Trehalase localization in the cerebral cortex, hippocampus and cerebellum of mouse brains. *J Adv Res* 18:71–79. <https://doi.org/10.1016/j.jare.2019.01.009>
77. Levine B, Packer M, Codogno P (2015) Development of autophagy inducers in clinical medicine. *J Clin Invest* 125(1):14–24. <https://doi.org/10.1172/JCI73938>
78. Li Y, Chen Y (2019) AMPK and Autophagy. *Adv Exp Med Biol* 1206:85–108. https://doi.org/10.1007/978-981-15-0602-4_4
79. Suzuki A, Okamoto S, Lee S, Saito K, Shiuchi T, Minokoshi Y (2007) Leptin stimulates fatty acid oxidation and peroxisome proliferator-activated receptor alpha gene expression in mouse C2C12 myoblasts by changing the subcellular localization of the alpha2 form of AMP-activated protein kinase. *Mol Cell Biol* 27(12):4317–4327. <https://doi.org/10.1128/MCB.02222-06>
80. Afinanisa Q, Cho MK, Seong HA (2021) AMPK Localization: a key to differential energy regulation. *Int J Mol Sci* 22(20). <https://doi.org/10.3390/ijms222010921>
81. Gao Q (2019) Oxidative stress and autophagy. *Adv Exp Med Biol* 1206:179–198. https://doi.org/10.1007/978-981-15-0602-4_9
82. Yang W, Tiffany-Castiglioni E (2008) Paraquat-induced apoptosis in human neuroblastoma SH-SY5Y cells: involvement of p53 and mitochondria. *J Toxicol Environ Health A* 71(4):289–299. <https://doi.org/10.1080/15287390701738467>
83. Lu M, Su C, Qiao C, Bian Y, Ding J, Hu G (2016) Metformin prevents dopaminergic neuron death in MPTP/P-induced mouse model of parkinson's disease via autophagy and mitochondrial ROS clearance. *Int J Neuropsychopharmacol* 19(9). <https://doi.org/10.1093/ijnp/pyw047>
84. Mizunoe Y, Kobayashi M, Sudo Y, Watanabe S, Yasukawa H, Natori D, Hoshino A, Negishi A, Okita N, Komatsu M, Higami Y (2018) Trehalose protects against oxidative stress by regulating the Keap1-Nrf2 and autophagy pathways. *Redox Biol* 15:115–124. <https://doi.org/10.1016/j.redox.2017.09.007>
85. Rodríguez-Navarro JA, Rodríguez L, Casarejos MJ, Solano RM, Gómez A, Perucho J, Cuervo AM, García de Yébenes J, Mena MA (2010) Trehalose ameliorates dopaminergic and tau pathology in parkin deleted/tau overexpressing mice through autophagy activation. *Neurobiol Dis* 39(3):423–438. <https://doi.org/10.1016/j.nbd.2010.05.014>
86. Orimo S, Uchihara T, Kanazawa T, Itoh Y, Wakabayashi K, Kakita A, Takahashi H (2011) Unmyelinated axons are more vulnerable to degeneration than myelinated axons of the cardiac nerve in Parkinson's disease. *Neuropathol Appl Neurobiol* 37(7):791–802. <https://doi.org/10.1111/j.1365-2990.2011.01194.x>
87. Braak H, Sandmann-Keil D, Gai W, Braak E (1999) Extensive axonal Lewy neurites in Parkinson's disease: a novel pathological feature revealed by alpha-synuclein immunocytochemistry. *Neurosci Lett* 265(1):67–69. [https://doi.org/10.1016/s0304-3940\(99\)00208-6](https://doi.org/10.1016/s0304-3940(99)00208-6)
88. Shih AY, Johnson DA, Wong G, Kraft AD, Jiang L, Erb H, Johnson JA, Murphy TH (2003) Coordinate regulation of glutathione biosynthesis and release by Nrf2-expressing glia potently protects neurons from oxidative stress. *J Neurosci* 23(8):3394–3406. <https://doi.org/10.1523/JNEUROSCI.23-08-03394.2003>
89. Chen Y, Vartiainen NE, Ying W, Chan PH, Koistinaho J, Swanson RA (2001) Astrocytes protect neurons from nitric oxide toxicity by a glutathione-dependent mechanism. *J Neurochem* 77(6):1601–1610. <https://doi.org/10.1046/j.1471-4159.2001.00374.x>
90. Tansey MG, Romero-Ramos M (2019) Immune system responses in Parkinson's disease: Early and dynamic. *Eur J Neurosci* 49(3):364–383. <https://doi.org/10.1111/ejn.14290>
91. Mehra S, Sahay S (1867) Maji SK (2019) α -Synuclein misfolding and aggregation: Implications in Parkinson's disease pathogenesis. *Biochim Biophys Acta Proteins Proteom* 10:890–908. <https://doi.org/10.1016/j.bbapap.2019.03.001>

Publisher's Note Springer Nature remains neutral with regard to jurisdictional claims in published maps and institutional affiliations.

Springer Nature or its licensor (e.g. a society or other partner) holds exclusive rights to this article under a publishing agreement with the author(s) or other rightsholder(s); author self-archiving of the accepted manuscript version of this article is solely governed by the terms of such publishing agreement and applicable law.